Mycobacterium tuberculosis requires conditionally essential metabolic pathways for infection

Alisha M. Block[1], Parker C. Wiegert[1], Sarah B. Namugenyi[1,#a], and Anna D. Tischler[1*]

[1] Department of Microbiology and Immunology, University of Minnesota, Twin Cities Campus, Minneapolis, MN, USA

[#a] Current Address: Infectious Disease Laboratory, Public Health Laboratory, Minnesota Department of Health, St. Paul, Minnesota, USA

* Corresponding author

E-mail: tischler@umn.edu (ADT)

Short title: *M. tuberculosis* metabolic pathways essential for infection

ABSTRACT

New drugs are needed to shorten and simplify treatment of tuberculosis caused by *Mycobacterium tuberculosis*. Metabolic pathways that *M. tuberculosis* requires for growth or survival during infection represent potential targets for anti-tubercular drug development. Genes and metabolic pathways essential for *M. tuberculosis* growth in standard laboratory culture conditions have been defined by genome-wide genetic screens. However, whether *M. tuberculosis* requires these essential genes during infection has not been comprehensively explored because mutant strains cannot be generated using standard methods. Here we show that *M. tuberculosis* requires functional phenylalanine (Phe) and *de novo* purine and thiamine biosynthetic pathways for mammalian infection. We used a defined collection of *M. tuberculosis* transposon (Tn) mutants in essential genes, which we generated using a custom nutrient-rich medium, and transposon sequencing (Tn-seq) to identify multiple central metabolic pathways required for fitness in a mouse infection model. We confirmed by individual retesting and complementation that mutations in *pheA* (Phe biosynthesis) or *purF* (purine and thiamine biosynthesis) cause death of *M. tuberculosis* in the absence of nutrient supplementation *in vitro* and strong attenuation in infected mice. Our findings show that Tn-seq with defined Tn mutant pools can be used to identify *M. tuberculosis* genes required during mouse lung infection. Our results also demonstrate that *M. tuberculosis* requires Phe and purine/thiamine biosynthesis for survival in the host, implicating these metabolic pathways as prime targets for the development of new antibiotics to combat tuberculosis.

AUTHOR SUMMARY

Mycobacterium tuberculosis causes more than 10 million new cases of active tuberculosis (TB) disease and 1.6 million deaths worldwide each year. Individuals with active TB must take a combination of four antibiotics for a minimum of 6-9 months to cure the infection. New anti-tubercular drugs are needed to simplify TB treatment and combat drug resistance. Here, we describe a novel collection of *M. tuberculosis* mutants lacking metabolic pathways essential for growth in standard laboratory conditions. Using these mutants, a mouse infection model, and deep sequencing we identified those

metabolic pathways that *M. tuberculosis* also requires during infection. We find that *M. tuberculosis* mutants that cannot synthesize purine nucleotides, riboflavin, or certain amino acids are unable to grow in mice. We also find that mutant strains which cannot synthesize purine nucleotides or the amino acid phenylalanine die rapidly in laboratory cultures without nutrient supplementation, suggesting that new drugs targeting these pathways would kill *M. tuberculosis*. Overall, our work reveals multiple metabolic pathways that *M. tuberculosis* requires during infection, which could be pursued as new targets for development of anti-tubercular drugs.

INTRODUCTION

Mycobacterium tuberculosis caused more deaths worldwide in 2021 than any other bacterial infectious agent, in part due to the complexity of tuberculosis (TB) treatment, which requires 6-9 months of therapy with multiple antibiotics [1, 2]. Multidrug-resistant *M. tuberculosis* (MDR-TB) accounts for ~4.2% of TB infections and is more challenging to treat, requiring use of less effective second-line agents [1, 3]. Development of new anti-tubercular drugs will be critical to reduce the length of TB treatment and to combat antibiotic resistance. New drug regimens hold some promise for reducing TB treatment duration and for treating MDR-TB [4-6]. However, defining diverse new targets for TB drug development will be necessary to counteract antibiotic resistance, which has already been documented for all existing drugs and all new or repurposed TB drugs in the clinical pipeline [7]. Metabolic pathways that *M. tuberculosis* requires for *in vitro* growth and that are highly vulnerable to inhibition have been proposed as novel TB drug targets [8-11]. However, these metabolic pathways may not be required for *M. tuberculosis* growth during infection due to differences in nutrient availability in host tissues as compared to the *in vitro* growth medium. Defining the metabolic pathways that *M. tuberculosis* requires during mammalian infection will be essential to prioritize targets for TB drug development.

M. tuberculosis genes required during mammalian infection have been defined by genome-wide transposon (Tn) mutant screens in the mouse infection model [12-17]. However, these studies excluded analysis of genes that are essential for *M. tuberculosis* growth in standard culture conditions *in vitro* [11], as it is not possible to generate

insertional mutations in these genes. In a few cases, auxotrophic *M. tuberculosis* mutant strains generated on medium supplemented with exogenous nutrients were used to demonstrate that specific central metabolic pathways are essential for growth in mice. These include pathways for synthesis of the amino acids Met, Arg, Pro and Trp [13, 18-21]. Other metabolic pathways such as coenzyme A, biotin, and trehalose synthesis were shown to be essential during mouse infection using *M. tuberculosis* conditional gene expression strains [22-24]. Each of these pathways are being pursued as potential targets for TB drug development.

However, not all metabolic pathways essential for *M. tuberculosis* growth *in vitro* are also required during mammalian infection. For example, the *nadABC* genes, which encode enzymes for *de novo* NAD+ synthesis, are essential *in vitro* but dispensable in the host [25, 26]. *M. tuberculosis* can scavenge the nicotinamide precursor from host tissue to synthesize NAD+ using an alternative salvage pathway [26]. This example highlights the importance of determining whether genes that *M. tuberculosis* requires for *in vitro* growth are also necessary during infection. Of the 625 genes annotated as essential for optimal growth of *M. tuberculosis* on standard Middlebrook medium [11], only a few have been directly tested to determine whether they are also required during infection because deletion mutant strains lacking these genes cannot be generated under standard culture conditions.

We previously developed an arrayed Tn mutant library using MtbYM rich medium, a custom medium that contains many additional carbon and nitrogen sources, amino acids, nucleotide precursors, co-factors and vitamins as compared to standard Middlebrook medium [27, 28]. Based on genome-wide transposon-sequencing (Tn-seq) analysis, 118 genes annotated as essential for optimal growth on Middlebrook 7H10 are non-essential on MtbYM rich [27]. These include genes required for synthesis of amino acids (Arg, Trp, Ile, Val, Leu, Glu, Pro, Ser, Tyr, Gln, Phe, Met, Cys), vitamins and co-factors (riboflavin, folates, pantothenate, NAD), and purine nucleotides, as well as certain catabolic pathways, including glycolysis [27]. We reasoned that our unique collection of Tn mutant strains selected on MtbYM rich medium could be exploited to rapidly assess whether *M. tuberculosis* requires these conditionally essential metabolic pathways for growth and survival during infection.

Here, we show that *M. tuberculosis* requires functional phenylalanine (Phe) biosynthesis and *de novo* purine nucleotide and thiamine biosynthesis pathways for growth in the mammalian host. We screened our collection of Tn mutants in conditionally essential genes in a mouse infection model using transposon sequencing (Tn-seq) and identified multiple central metabolic pathways that *M. tuberculosis* requires for fitness in host lung and spleen tissues. We confirm that mutation of *pheA* (Phe synthesis) or *purF* (purine/thiamine synthesis) causes death of *M. tuberculosis* in the absence of exogenous nutrient supplementation *in vitro* and in the lungs of aerosol-infected mice. Our results demonstrate roles for multiple metabolic pathways in *M. tuberculosis* fitness during infection and implicate the Phe and purine/thiamine biosynthetic pathways as novel targets for development of anti-tubercular drugs.

RESULTS

M. tuberculosis genes that are essential for growth in standard Middlebrook medium have been defined by saturating Tn mutagenesis screens [11]. We previously constructed an arrayed Tn mutant library in the *M. tuberculosis* Erdman strain using MtbYM rich medium, which contains many additional carbon sources, amino acids, metabolic intermediates, vitamins and co-factors that are not present in Middlebrook medium [27, 28]. Our library contains 48 Tn mutants in genes annotated as “essential” in Middlebrook medium that are non-essential in MtbYM rich medium [11, 27, 28]. We refer to these genes as Middlebrook-Essential (M-ES) genes. To determine whether *M. tuberculosis* requires these M-ES genes for survival in the host, we isolated Tn mutants in M-ES genes from our arrayed library and screened them for fitness defects in mice using transposon sequencing (Tn-seq).

Tn insertions in genes annotated as essential for growth on Middlebrook medium can be isolated on MtbYM rich medium.

Our arrayed *M. tuberculosis* Erdman Tn library made on MtbYM rich medium contains a total of 105 unique Tn insertions in 48 M-ES genes (**S1 Table**). Of these, 20 mutants in 17 unique M-ES genes harbored the Tn insertion near the 5’ or 3’ end of the gene (within the first 5% or last 95% of the coding sequence). As these Tn insertions were unlikely to disrupt gene function, these mutants were excluded from this study

139 (**S1C Table**, Tn mutants excluded). We recovered 45 of the Tn mutants in M-ES genes
140 from their mapped locations in our arrayed library on MtbYM rich agar and confirmed
141 the Tn insertion site by PCR (**S1A and S1B Table**).
142 We previously determined that some mutants in our MtbYM rich Tn library have
143 defects in production of the outer membrane lipid phthiocerol dimycocerosate (PDIM)
144 due to secondary mutations, unlinked to the Tn [28]. The M-ES Tn mutants might be
145 PDIM deficient due to similar secondary mutations. As *M. tuberculosis* requires PDIM
146 for virulence [17], we confirmed that the M-ES Tn mutants were PDIM-proficient prior to
147 screening for fitness defects in mice. We used PCR and Sanger sequencing to test the
148 M-ES Tn mutants for point mutations in PDIM biosynthesis genes that we identified in
149 other Tn mutants from our library. This analysis identified 6 M-ES Tn mutants with
150 mutations in genes required for PDIM production (**S1B Table**, unusable Tn mutants).
151 We conducted whole genome sequencing on the remaining M-ES Tn mutants, which
152 identified additional mutations predicted to prevent PDIM production in 17 Tn mutants
153 and one mutant with multiple Tn insertions (**S1B Table**, unusable Tn mutants). These
154 mutants were excluded from further analysis. We recovered Tn mutants in 19 M-ES
155 genes which contained a single Tn insertion and no mutations in genes required for
156 PDIM production, based on whole genome sequencing (**S1A Table**, Tn mutants in M-
157 ES library). These M-ES Tn mutants, representing various metabolic pathways and
158 essential processes (**Table 1**), were selected for analysis of growth *in vitro* and fitness
159 defects in mice.
160 **Table 1. Tn mutants in M-ES genes in the Tn library screened in mice.**

Gene	Annotation	Putative Function
purF	amidophosphoriboysltransferase	*de novo* purine & thiamine biosynthesis
purM	phosphoribosyl-aminoimidazole synthase	*de novo* purine & thiamine synthesis
purQ	phosphoribosyl-formylglycinamidine synthetase I	*de novo* purine & thiamine synthesis
pheA	prephenate dehydratase	Phe biosynthesis
trpG	anthranilate synthase component II	Trp biosynthesis
trpB	tryptophan synthase beta chain	Trp biosynthesis
proC	pyrroline-5-carboxylate reductase	Pro biosynthesis
gltB	ferredoxin-dependent glutamate synthetase	Glu biosynthesis

ilvA	threonine dehydratase	Ile biosynthesis
panC	pantoate-beta-alanine ligase	pantothenate biosynthesis
ribA2	GTP cyclohydrolase II	riboflavin biosynthesis
ribG	bifunctional riboflavin synthesis protein	riboflavin biosynthesis
pabB	*para*-aminobenzoic acid (PABA) synthase component I	PABA biosynthesis
fhaA	conserved protein with forkhead-associated domain	regulation of cell wall synthesis
pstP	serine-threonine phosphatase	regulation of cell wall synthesis
ftsQ	cell division protein	cell division
ERDMAN_3321	possible acyl transferase	unknown function
ERDMAN_2739	Obg GTPase	ribosome assembly
ERDMAN_4254	LigA DNA ligase	DNA damage repair

Tn mutants in central metabolic pathways have growth defects in Middlebrook 7H9 medium.

To determine whether the M-ES genes disrupted by Tn insertion are required for *M. tuberculosis* growth in standard culture conditions, we conducted growth curves in Middlebrook 7H9 medium. Tn mutants in genes encoding various central metabolic pathway enzymes exhibited severe growth defects. These included Tn mutants in genes required for purine and thiamine biosynthesis (*purF*, *purM*, *purQ*; **Fig 1A**), biosynthesis of the amino acids Phe, Trp, Pro, Glu and Ile (*pheA*, *trpB*, *trpG*, *proC*, *gltB*, *ilvA*; **Figs 1B and 1C**), and riboflavin or *para*-amino benozoic acid (PABA) biosynthesis (*ribA2*, *ribG*, *pabB*; **Fig 1D**). The *panC*::Tn mutant was included in our study as a positive control, and as expected it also failed to grow in Middlebrook 7H9 (**Fig 1D**). *M. tuberculosis* requires PanC for synthesis of pantothenate (vitamin B5), an essential precursor in coenzyme A biosynthesis, in the absence of exogenous pantothenate [29]. These data demonstrate that each of these M-ES genes is essential for growth of *M. tuberculosis* Erdman in standard Middlebook medium, consistent with their annotation as essential for growth on Middlebrook 7H10 based on saturating Tn mutagenesis [11].

Tn mutants in several other putative M-ES genes had no growth defects in 7H9 (**Figs 1E and 1F**). Four Tn mutants harbored insertions within non-essential domains of M-ES genes. PstP and FhaA regulate *M. tuberculosis* cell wall synthesis [30, 31] and have domains predicted to be non-essential by saturating Tn mutagenesis [11]. The *pstP*::Tn and *fhaA*::Tn mutants both harbor the Tn insertion in a non-essential region of

183 the gene and grew normally (**Fig 1E**). *M. tuberculosis* requires the membrane protein
184 FtsQ to regulate cell division [32]. Our *ftsQ*::Tn mutant harbors the Tn at 185 bp from
185 the 5' end, in a region predicted to be non-essential [11]. The *ftsQ*::Tn mutant exhibited
186 no growth defect (**Fig 1E**), suggesting that truncated FtsQ lacking 62 amino acids of the
187 N-terminal cytosolic domain can sustain normal cell division *in vitro.* Our data are
188 consistent with the observation that the FtsQ periplasmic domain complements the cell
189 division defects of an FtsQ-depleted strain [32]. *ERDMAN_3321* (*rv3034*), which
190 encodes a putative acetyl transferase, is annotated as essential, but Tn insertions near
191 the 5' end of the gene confer a growth advantage [11]. The *ERDMAN_3321*::Tn mutant
192 harbors the Tn insertion 151 bp from the 5' end of the gene, within this non-essential
193 region (**Fig 1F**).
194 We also isolated two mutants with Tn insertions in *M. tuberculosis* Erdman genes
195 with annotations suggesting essentiality. *ERDMAN_2739* is annotated as *obg* [33]; in *M.*
196 *tuberculosis* H37Rv *obgE* (r*v2440c*) encodes an essential GTPase that controls
197 ribosome assembly [11, 34, 35]. *ERDMAN_4254* is annotated as a DNA ligase [33], with
198 possible similarity to the essential DNA ligase *ligA* (*rv3014*) [11]. Whole genome
199 sequencing revealed that the *ERDMAN_2739*::Tn insertion is within *pe_pgrs43* and the
200 *ERDMAN_4254*::Tn insertion is within *espK*, both of which are non-essential genes [11].
201 Thus, it is not surprising that these mutants did not exhibit growth defects (**Fig 1F**).
202 These data indicate that a subset of the Tn mutants we isolated do not disrupt functions
203 essential for *M. tuberculosis* growth in standard Middlebrook medium.
204 ***M. tuberculosis* requires many central metabolic pathways for fitness in mice.**
205 To identify those M-ES Tn mutants with fitness defects in mice, we created and
206 screened a library of Tn mutants in M-ES genes (**S1A Table**). We included in the M-ES
207 Tn library five positive control Tn mutants in genes known to be required for *M.*
208 *tuberculosis* fitness in mice: *panC*::Tn [29] and four independent Tn insertions in *phoP*,
209 which encodes a response regulator essential for virulence [36, 37]. We also included
210 five negative control Tn mutants in genes known to be dispensable for *M. tuberculosis*
211 growth and survival in mice: *rpfA* and *rpfE* that encode redundant resuscitation
212 promoting factors [38], *pstB* and *pstC1* that encode subunits of an alternate Pst
213 phosphate transporter [39], and *tadA* that encodes a Flp pilin assembly ATPase [40].

214 Each of these negative control Tn mutants were predicted to be PDIM-proficient based
215 on whole genome sequencing (**S1A Table**). The Tn mutants were grown individually in
216 MtbYM rich liquid medium and equivalent amounts of each mutant were combined to
217 generate the M-ES Tn library (**Fig 2A**). Bacteria in the M-ES Tn library were collected in
218 triplicate for genomic DNA extraction as a control to confirm equal representation of
219 each Tn mutant and aliquots of the library were frozen for use in experiments (**Fig 2A**).
220 To screen the M-ES Tn library for fitness defects in mice, the library was grown in
221 MtbYM rich liquid, pelleted in triplicate for genomic DNA extraction as an input control
222 (Liquid control), plated on MtbYM rich agar as a control for recovery on plates (Plate
223 control), and used to infect C57BL/6J mice by intravenous injection (**Fig 2A**). The
224 intravenous route was used to ensure adequate representation of all Tn mutants in both
225 lung and spleen tissues. At days 1, 7, 21 and 42 post-infection, groups of mice (*n*=3)
226 were euthanized and surviving *M. tuberculosis* CFU were recovered from lung and
227 spleen homogenates by plating on MtbYM rich agar (**Fig 2A**). We noted high variability
228 in *M. tuberculosis* CFU recovered from the lungs at days 7 and 42 (**Fig 2B**). For
229 analysis of Tn mutant fitness by Tn-seq, we selected plates containing at least 10^4 *M.*
230 *tuberculosis* CFU for genomic DNA extraction. Since only one mouse each at the day 7
231 and day 42 time points had sufficient CFU in the lungs for Tn-seq analysis (**Fig 2B**), the
232 lung samples were analyzed only at days 1 and 21. Sufficient bacteria were recovered
233 from the spleens at all time points for Tn-seq analysis (**Fig 2B**).
234 To determine Tn mutant fitness, the triplicate genomic DNA samples from the
235 library input, liquid input, plate input, and tissue homogenates plated on MtbYM rich
236 agar (**Fig 2A**) were subjected to Tn-seq analysis and read counts for each Tn insertion
237 site were tabulated (**S2 Table**). To determine relative Tn mutant fitness, we used
238 TnseqDiff, which identifies conditionally essential genes between conditions based on
239 the relative frequencies of Tn-seq sequencing reads at each Tn insertion site [41]. We
240 previously used this approach to identify Tn mutants with altered fitness in low-
241 complexity *M. tuberculosis* Tn mutant libraries treated with antibiotics *in vitro* [28].
242 Complete TnseqDiff analyses are provided in **S3 Table**.
243 No statistically significant fitness defects were observed in comparisons between
244 the original M-ES Tn library and the MtbYM rich liquid culture that was used to infect the

245 mice (**Fig 2C**, **S1A Fig**), suggesting that all Tn mutants grow equally well in MtbYM rich
246 medium. In TnseqDiff comparisons between the original M-ES Tn library and the input
247 plated on MtbYM rich agar, several M-ES Tn mutants showed slight, but statistically
248 significant fitness defects (*purF*::Tn, *purM*::Tn, *purQ*::Tn, *gltB*::Tn, *panC*::Tn; **Fig 2C**,
249 **S1B Fig**). These Tn mutants may have growth defects on MtbYM rich agar compared to
250 other mutants in the M-ES Tn library, which causes their under-representation after
251 recovery on plates. These data suggest that most M-ES Tn mutants are efficiently
252 recovered on MtbYM rich agar and that any fitness defects observed following mouse
253 infection are due to inability to survive within the mouse rather than a competitive
254 disadvantage on MtbYM rich agar.

255 To determine relative Tn mutant fitness at day 1 post-infection, we compared Tn
256 mutant abundance in plated mouse tissues to the input plated on MtbYM agar (D1
257 lungs/plate or D1 spleen/plate) using TnseqDiff. Three Tn mutants (*gltB*::Tn, *pheA*::Tn,
258 *panC*::Tn) were significantly under-represented in the lungs at day 1 post-infection (**Figs**
259 **2C and 2D**). Attenuation of *panC*::Tn was expected, as *panC* was essential for *M.*
260 *tuberculosis* growth in BALB/c mice [29]. We observed similarly reduced fitness of the
261 *gltB*::Tn and *pheA*::Tn mutants in the spleen at day 1 post-infection (**Fig 2C**, **S1C Fig**).
262 These data suggest that Phe biosynthesis (PheA) and Glu biosynthesis (GltB) are
263 essential for *M. tuberculosis* survival within host tissues at the earliest stage of infection.

264 To determine Tn mutant fitness in the lungs and spleens at later times post-
265 infection, the day 7, day 21 or day 42 outputs were compared to the day 1 input from
266 the corresponding tissue using TnseqDiff. We identified 14 Tn mutants that exhibited
267 significantly reduced fitness in the lungs at day 21 post-infection (**Figs 2C and 2E**).
268 These included Tn mutants in genes encoding enzymes required for purine and
269 thiamine biosynthesis (*purF*::Tn, *purM*::Tn, *purQ*::Tn), amino acid biosynthesis
270 (*pheA*::Tn, *trpB*::Tn, *trpG*::Tn, *proC*::Tn), riboflavin synthesis (*ribA2*::Tn, *ribG*::Tn) and
271 PABA synthesis (*pabB*::Tn), as well as the *panC*::Tn and *phoP*::Tn positive controls.
272 Attenuation of the *trpB*::Tn and *trpG*::Tn mutants was expected as another gene in the
273 Trp biosynthesis pathway (*trpE*) was previously implicated in *M. tuberculosis* growth in
274 C57BL/6 mice [13].

275 We observed a similar pattern of attenuation in the spleens at day 21. Most Tn
276 mutants that were attenuated in lungs also exhibited significant fitness defects in the
277 spleen (**Figs 2C and 2F**). One exception is *pabB*::Tn, which was significantly attenuated
278 in lungs but not spleens (**Figs 2C, 2E and 2F**). The Tn mutants that exhibited significant
279 fitness defects in the spleen at day 21 were also significantly attenuated in the spleen at
280 days 7 and 42 post-infection (**Fig 2C; S1D and S1E Figs**). The *pheA*::Tn mutant was
281 significantly attenuated in lungs and spleens at all time points, despite significantly
282 reduced fitness at day 1 (**Fig 2C**). In contrast, the *gltB*::Tn mutant was attenuated in
283 lungs and spleens, but this did not achieve statistical significance, possibly because the
284 *gltB*::Tn mutant was at much lower abundance in the day 1 normalization controls (**Fig**
285 **2C, S1C Fig**). Overall, these data suggest that *M. tuberculosis* requires multiple central
286 metabolic pathways, particularly purine nucleotide and thiamine biosynthesis, riboflavin
287 biosynthesis, and biosynthesis of specific amino acids (Phe, Trp, Pro, Glu) to replicate
288 within host tissues.
289 While most M-ES Tn mutants with *in vitro* growth defects were attenuated in
290 mice, the *ilvA*::Tn mutant was a notable exception. The *ilvA*::Tn mutant did not replicate
291 in Middlebrook 7H9 *in vitro* (**Fig 1C**), but exhibited no statistically significant fitness
292 defects in mouse lungs or spleens at any time point (**Fig 2C**). These data indicate that
293 *M. tuberculosis* does not require the *de novo* Ile biosynthesis during mouse infection
294 and suggest that it can acquire sufficient Ile from the host.
295 **Purine and thiamine auxotrophy is cidal for *M. tuberculosis in vitro* and in mice.**
296 To confirm the results of our Tn-seq screen, we selected two Tn mutants for
297 individual retesting. We selected *purF*::Tn as a representative mutant with defects in
298 biosynthesis of purine and thiamine. PurF catalyzes the first committed step of *de novo*
299 purine nucleotide biosynthesis, which also produces a metabolic precursor required for
300 the *de novo* synthesis of thiamine (vitamin B1) (**Fig 3A**) [42]. In *M. tuberculosis*, purine
301 nucleotides can be produced either *de novo* or via a salvage pathway from
302 hypoxanthine, which is converted to the purine nucleotide precursor inosine
303 monophosphate (IMP) by hypoxanthine-guanine phosphoribosyltransferase (Hpt) [43].
304 We confirmed that the *purF*::Tn mutant fails to grow in standard Middlebrook 7H9
305 medium and that the growth defect can be alleviated with exogenous hypoxanthine and

306 thiamine (**Fig 3B**), the two components of MtbYM rich predicted to bypass *de novo*
307 purine biosynthesis [27]. Exogenous hypoxanthine alone partially rescued growth of the
308 *purF*::Tn mutant, but full growth restoration only occurred with both nutrients added (**S2**
309 **Fig**). The growth defect of the *purF*::Tn mutant in 7H9 was also fully complemented by
310 *purF* expressed from a plasmid (pMV-*purF*, **Fig 3B**). The *purF*::Tn mutant lost viability in
311 unsupplemented 7H9, with viable CFU below the limit of detection (1 CFU/ml) after 21
312 days of incubation (**Fig 3C**). Viability of the *purF*::Tn mutant was restored by either
313 exogenous hypoxanthine and thiamine or by complementation with pMV-*purF* (**Fig 3C**).
314 These data demonstrate that loss of PurF function causes death of *M. tuberculosis* in
315 the absence of nutrient supplementation.
316 To determine if *M. tuberculosis* requires PurF during infection, we infected
317 C57BL/6J mice by aerosol with WT Erdman, *purF*::Tn or the *purF*::Tn pMV-*purF*
318 complemented strain. All strains were confirmed to produce the PDIM lipid that is
319 essential for virulence using thin layer chromatography of ^{14}C-propionate labelled lipid
320 extracts (**S3 Fig**). The *purF*::Tn mutant established infection in the lungs at day 1 post-
321 infection, but it failed to replicate, was cleared from the lungs by day 42 post-infection,
322 and failed to disseminate to the spleen (**Figs 3D and 3E**). Attenuation of the *purF*::Tn
323 mutant was partially complemented by pMV-*purF*. The *purF*::Tn pMV-*purF* strain
324 replicated in the lungs and disseminated to spleen, but significantly fewer CFU were
325 recovered compared to the WT control (**Figs 3D and 3E**). Expression of *purF* from the
326 pMV-*purF* plasmid may be insufficient to support *M. tuberculosis* growth in host tissues.
327 Alternatively, the *purF*::Tn insertion may be polar on the 3' *purM* gene, which is also a
328 M-ES gene [11]. Reduced expression of *purF* or *purM* could prevent normal *M.*
329 *tuberculosis* replication in mice, in which demand for purine nucleotides and/or thiamine
330 may be higher as compared to *in vitro* culture. Overall, our data demonstrate that the Tn
331 insertion in *purF*, not a secondary mutation, causes attenuation in mice. These data
332 indicate that *M. tuberculosis* cannot obtain sufficient purine nucleotide precursors and/or
333 thiamine to support growth in host tissues and implicate the purine and thiamine
334 biosynthetic pathways as TB drug targets.
335 ***M. tuberculosis* requires Phe biosynthesis for survival *in vitro* and in mice.**

336 We selected the *pheA*::Tn mutant for retesting as the role of Phe biosynthesis in
337 *M. tuberculosis* fitness either *in vitro* or in the host has not previously been tested and
338 the Phe biosynthesis pathway is absent in humans, making it an attractive drug target
339 [44]. PheA is a prephenate dehydratase required for both pathways of Phe synthesis
340 (**Fig 4A**). PheA catalyzes the first step in Phe synthesis from prephenate [45], which is
341 produced from chorismate by chorismate mutase [44]. Two *M. tuberculosis* proteins
342 have chorismate mutase activity (Rv1885c and Rv0948c), but Rv1885c is secreted
343 while Rv0948c is cytosolic [46-48]. Only *rv0948c* is a M-ES gene [11], suggesting that it
344 functions as the chorismate mutase in Phe synthesis. In plants and some bacteria, Phe
345 synthesis can also proceed via an L-arogenate intermediate [44]. L-arogenate has been
346 detected in *M. tuberculosis* [49], and the aminotransferase Rv1178c may synthesize L-
347 arogenate from chorismate, as this enzyme activity has been demonstrated *in vitro* [50].
348 PheA is predicted to act as the dehydratase to convert L-arogenate to Phe.
349 We confirmed that the *pheA*::Tn mutant does not grow in 7H9 medium unless the
350 medium is supplemented with casamino acids, which contains Phe (**Fig 4B**). The
351 growth defect of the *pheA*::Tn mutant in 7H9 was also fully complemented with plasmid-
352 encoded *pheA* (pMV-*pheA*, **Fig 4B**). The *pheA*::Tn mutant also lost viability in 7H9 in
353 the absence of casamino acid supplementation, indicating that an inability to acquire or
354 produce Phe is cidal to *M. tuberculosis* (**Fig 4C**). This survival defect was also fully
355 complemented by pMV-*pheA* (**Fig 4C**). These data demonstrate that blocking Phe
356 synthesis causes death of *M. tuberculosis* in the absence of exogenous nutrient
357 supplementation.
358 To confirm attenuation of the *pheA*::Tn mutant, C57BL/6J mice were infected by
359 aerosol with WT Erdman, *pheA*::Tn, or the *pheA*::Tn pMV-*pheA* complemented strain.
360 The *pheA*::Tn and *pheA*::Tn pMV-*pheA* strains both produce the PDIM lipid (**Fig S3**).
361 Despite using a higher inoculating dose, we observed significantly fewer *pheA*::Tn
362 bacteria in the lungs at 24 hr post-infection compared to either the WT or complemented
363 controls (**Fig 4D**). This is consistent with the significant reduction in fitness we observed
364 for the *pheA*::Tn mutant at day 1 post-infection compared to the plated input control in
365 our Tn-seq screen (**Figs 2C & 2D**). These data suggest that PheA is required for *M.*
366 *tuberculosis* to establish infection in the lungs. The *pheA*::Tn mutant was also incapable

367 of replicating in mouse lungs, was cleared to below the limit of detection from lung
368 tissues by 42 days post-infection, and failed to disseminate to the spleen (**Figs 4D &**
369 **4E**). The *pheA*::Tn pMV-*pheA* complemented strain replicated in the lungs (**Fig 4D**) and
370 disseminated to spleen (**Fig 4E**) similarly to the WT control. These data show that
371 attenuation of the *pheA*::Tn mutant is due to the Tn insertion in *pheA* and not a
372 secondary mutation. These data also demonstrate that *M. tuberculosis* requires Phe
373 biosynthesis to survive within the host, suggest that Phe is not available in sufficient
374 quantities in host tissues to support *M. tuberculosis* growth, and indicate that PheA is a
375 potential target for development of new TB drugs.
376

377 **DISCUSSION**

378 Most metabolic pathways that are essential for *M. tuberculosis* growth in
379 standard *in vitro* culture conditions have not previously been evaluated to determine
380 their importance during infection because mutant strains lacking these metabolic
381 functions cannot be generated using standard methods. Here we use a Tn mutant
382 collection generated using a nutrient-enriched growth medium to demonstrate that
383 several metabolic pathways essential for growth in standard *in vitro* culture conditions
384 are also essential in the host using a mouse infection model. Our data show that *M.*
385 *tuberculosis* requires *de novo* purine and thiamine biosynthesis as well as Phe
386 biosynthesis for replication in the lungs and dissemination to the spleen in aerosol-
387 infected mice. In addition, we show that an inability to synthesize Phe or purine and
388 thiamine causes death of *M. tuberculosis* in the absence of exogenous nutrients,
389 suggesting that inhibitors of these biosynthetic pathways would be bacteriocidal.
390 Therefore, our data implicate the Phe and purine/thiamine biosynthesis pathways as
391 promising targets for development of novel anti-tubercular drugs.

392 Phe biosynthesis has been explored as a target for anti-tubercular drug
393 development because mammals lack *de novo* Phe synthesis, which is expected to limit
394 the toxicity of compounds targeting this pathway [44]. Our data support PheA as a
395 potential drug target since our *pheA*::Tn mutant exhibited strong attenuation in the
396 mouse model, suggesting that *M. tuberculosis* cannot acquire sufficient Phe from the
397 host. Phe biosynthesis also requires conversion of chorismate to prephenate by

398 chorismate mutase [44]. Inhibitors of *M. tuberculosis* chorismate mutase have been
399 identified, but most of these compounds had high minimal inhibitory concentrations
400 (MICs), suggesting that they have low whole cell permeability [51-53]. Our data suggest
401 that *M. tuberculosis* can import Phe, since growth of the *pheA*::Tn mutant *in vitro* was
402 restored by amino acid supplementation. Therefore, it may be possible to design PheA
403 or chorismate mutase inhibitors with improved permeability properties for use as anti-
404 tubercular agents.

405 Purine nucleotide biosynthesis is critical for the virulence of many pathogens and
406 has also been explored as a drug development target [54]. Although mammals also
407 synthesize purine nucleotides *de novo*, the enzymes are structurally distinct, suggesting
408 that specific inhibitors of bacterial enzymes can be designed [42]. Our data demonstrate
409 that *M. tuberculosis* requires PurF, which catalyzes the first committed step of *de novo*
410 purine nucleotide and thiamine co-factor biosynthesis, for growth in the host. Our data
411 suggest that both purine and thiamine biosynthesis are critical functions of PurF, as *in*
412 *vitro* growth was fully restored only by adding exogenous thiamine and hypoxanthine.
413 Attenuation of the *purF*::Tn mutant in mice was only partially reversed by
414 complementation, despite full restoration of *in vitro* growth in the absence of nutrient
415 supplementation. This suggests that the demand for purine and/or thiamine
416 biosynthesis is greater within host tissues and that even partial loss of PurF function can
417 limit *M. tuberculosis* growth. Collectively, our data suggest that *M. tuberculosis* cannot
418 acquire sufficient purine nucleotides and/or thiamine from host tissues to support its
419 growth.

420 Our data also indicate that *M. tuberculosis* requires other enzymes in the purine
421 and thiamine biosynthetic pathway for growth in the host, as *purM*::Tn and *purQ*::Tn
422 mutants were highly attenuated in our Tn-seq screen. Our data are consistent with a
423 prior report that a *M. tuberculosis purC* mutant was cleared from the tissues of
424 intravenously-infected mice [55]. Our data are also consistent with the observation that
425 depletion of GuaB2, which is required for *de novo* synthesis of guanine nucleotides,
426 prevents *M. tuberculosis* replication in aerosol-infected mice [56]. Loss of either PurC or
427 GuaB2 function is predicted to prevent production of guanine nucleotides, but not
428 thiamine. Whether an inability to produce thiamine contributes to the attenuation of the

429 *purF*::Tn mutant remains to be determined. In addition, it is unclear whether *M.*
430 *tuberculosis* requires *de novo* purine and/or thiamine synthesis only for replication
431 during acute infection or also for persistence in host tissues during chronic infection.
432 Our future studies will explore these questions using *M. tuberculosis* strains that
433 conditionally express enzymes specific to the thiamine or purine biosynthetic pathways
434 or that are required for both pathways, like PurF. Overall, our data are consistent with
435 prior studies indicating that *M. tuberculosis* requires *de novo* purine biosynthesis for
436 growth in the host and support further development of inhibitors targeting this pathway.
437 Nucleotide synthesis inhibitors, which include approved cancer
438 chemotherapeutics, have shown efficacy against other bacterial pathogens, but can be
439 toxic to mammalian cells [54]. Structures of *M. tuberculosis* PurN, PurH, and PurF,
440 which are involved in *de novo* purine synthesis, revealed structural distinctions from the
441 equivalent human enzymes, suggesting that specific inhibitors could be designed
442 against these proteins [57-59]. *Mycobacterium abscessus* PurC is also structurally
443 distinct from the human ortholog, and PurC inhibitors that prevent *M. tuberculosis*
444 growth *in vitro* were recently described [60]. An indazole sulfonamide compound that
445 inhibits GuaB2 was cidal against replicating *M. tuberculosis in vitro* but lacked activity in
446 infected mice due to either low drug concentration in lung lesions, slower growth of *M.*
447 *tuberculosis* in chronically infected mice, or high levels of guanine in host tissues that
448 antagonize the drug [61]. It may be possible to develop improved drugs targeting other
449 enzymes in the purine biosynthetic pathway that would disrupt both purine and thiamine
450 biosynthesis. As *de novo* purine biosynthesis includes 10 enzymatic steps, it represents
451 a pathway rich in targets for the development of novel anti-tubercular agents.
452 The *de novo* thiamine biosynthesis pathway is also a promising target for
453 development of novel antimicrobials given that it is absent in humans, who must obtain
454 thiamine in the diet [62]. Inhibitors of thiamine biosynthesis with *in vitro* efficacy have
455 been reported for *Salmonella* and *Pseudomonas* [63, 64]. Inhibitors of *M. tuberculosis*
456 ThiE, which catalyzes the final step in production of the active co-enzyme thiamine
457 pyrophosphate, have also been identified, one of which potently inhibited *in vitro* growth
458 [65]. However, this study did not test whether the compound specifically targeted ThiE
459 through either selection of resistant mutants or use of hyper-morphic strains with

460 reduced ThiE expression. Further studies will be needed to determine if *M. tuberculosis*
461 requires thiamine synthesis during infection and to identify the steps in the biosynthetic
462 pathway that are most vulnerable to inhibition.

463 Loss of either PheA or PurF function causes rapid death of *M. tuberculosis* in the
464 absence of exogenous nutrient supplementation, suggesting that inhibitors targeting
465 these enzymes would be bacteriocidal. The *pheA*::Tn mutant died *in vitro* at a rate
466 comparable to a methionine auxotroph (Δ*metA*) without amino acid supplementation
467 [18]. The *purF*::Tn mutant was sterilized to below the limit of detection after only 21 days
468 of culture without hypoxanthine and thiamine. This is a faster rate of death in the
469 absence of nutrient supplementation than any other auxotrophic *M. tuberculosis* strains
470 that have been characterized, including Arg biosynthesis mutants, which are sterilized
471 by Arg deprivation [18, 19]. However, the molecular mechanisms that cause death of
472 either the *pheA*::Tn or *purF*::Tn mutants remain to be determined.

473 For other auxotrophic *M. tuberculosis* mutants, loss of viability was correlated
474 with multiple effects on microbial physiology. For example, the Δ*metA* mutant cannot
475 produce either Met or *S*-adenosylmethionine (SAM), an essential co-factor in one-
476 carbon metabolism [18]. Similarly, death of Arg biosynthesis mutants deprived of Arg
477 was correlated with increased production of endogenous reactive oxygen species and
478 DNA damage, in addition to reduced intracellular Arg [19]. Reduced Phe production in
479 the *pheA*::Tn mutant may deplete chorismate because chorismate mutase is feedback
480 inhibited by Phe [66]. Chorismate is also required as a precursor for synthesis of Trp,
481 menaquinones and the mycobactin siderophore, so its depletion would be expected to
482 affect multiple processes [47]. Loss of PurF function may be cidal in the absence of
483 nutrient supplementation due to reduced production of both purine nucleotides, which
484 are needed for DNA synthesis, RNA synthesis and energy storage [54], and thiamine,
485 which is needed for activity of multiple enzymes involved in central carbon metabolism
486 and branched chain amino acid biosynthesis [62]. Alternatively, the *purF*::Tn mutant
487 may be hypersusceptible to exogenous stress, including oxygen limitation, as previously
488 reported for a *Mycobacterium smegmatis purF* mutant [67]. The mechanisms by which
489 these mutations cause death of *M. tuberculosis* will be explored in our future studies.

490 In addition to the *purF*::Tn and *pheA*::Tn mutants that we selected for follow-up
491 studies, we identified several other Tn mutants that exhibited strong fitness defects in
492 mice. These included Tn insertions in genes required for riboflavin synthesis (*ribA2*,
493 *ribG*), PABA synthesis (*pabB*), and synthesis of the amino acids Pro and Glu (*proC,*
494 *gltB*). Our data suggest that *M. tuberculosis* cannot acquire these nutrients in sufficient
495 quantities from host tissues and must synthesize them *de novo*. To prioritize these
496 conditionally essential metabolic pathways as targets for drug development, we will
497 consider whether the pathway is present in mammalian cells, whether loss of the
498 pathway is cidal *in vitro* in the absence of nutrient supplementation, and whether the
499 pathway is vulnerable to inhibition.
500 Riboflavin, Glu and PABA synthesis pathways are absent from mammalian cells,
501 so compounds targeting these pathways would be expected to have low toxicity. We
502 can use our Tn mutants to assess whether starvation for these nutrients is cidal for *M.*
503 *tuberculosis in vitro*, as we have done for the *pheA*::Tn and *purF*::Tn mutants. PABA is a
504 metabolic precursor in folate biosynthesis. A *M. tuberculosis* PabB inhibitor has been
505 reported to overcome resistance to anti-folate drugs [68], indicating that compounds
506 targeting PabB can be developed. Vulnerability of *M. tuberculosis* to loss of gene
507 function *in vitro* has been estimated based upon reduced fitness with transcriptional
508 inhibition using CRISPR interference (CRISPRi) [9]. A genome-wide CRISPRi screen
509 revealed that *ribA2* and *gltB* were among the genes most vulnerable to inhibition, with
510 vulnerability indices in the top 4% of all of *M. tuberculosis* genes [9]. Many other M-ES
511 genes that we analyzed including *pheA*, *purF* and other genes required for purine
512 biosynthesis were also highly vulnerable, with vulnerability indices similar to the targets
513 of existing anti-TB drugs [9]. Our data indicate that riboflavin, Glu and PABA synthesis
514 are all required for acute *M. tuberculosis* infection and should be considered as potential
515 targets for development of new anti-tubercular agents. Future studies will address
516 whether these genes are also essential during chronic *M. tuberculosis* infection using
517 conditional expression strains.
518 While our data indicate that *M. tuberculosis* requires most of the M-ES genes that
519 we analyzed for survival in mice, *ilvA* was an exception. IlvA catalyzes the first step in
520 *de novo* synthesis of isoleucine (Ile), a branched chain amino acid (BCAA) [69]. BCAA

521 biosynthesis has been actively investigated as a target for antimicrobial development
522 because these pathways are absent in mammals [70]. In addition, *M. tuberculosis ilvA* is
523 highly vulnerable to inhibition *in vitro* [9]. However, our data suggest that IlvA would be a
524 poor drug target because the *ilvA*::Tn mutant was not attenuated in mice, despite strong
525 *in vitro* growth inhibition. Our data suggest that *M. tuberculosis* can obtain sufficient Ile
526 from host tissues to support its growth. Our data are consistent with the observation that
527 a *M. tuberculosis* mutant lacking *ilvB1*, which is required for synthesis of all BCAAs (Ile,
528 Leu, Val), was not cleared from lung or spleen tissues in intravenously-infected mice,
529 despite loss of viability *in vitro* without exogenous BCAA [71]. Indeed *M. tuberculosis*
530 can acquire all BCAAs directly from infected macrophages [72]. Our data highlight the
531 importance of directly testing whether the biosynthetic pathways essential for *in vitro*
532 growth are also necessary during infection prior to pursuing these pathways as drug
533 development targets.

534 Finally, our work highlights a new strategy for identifying *M. tuberculosis* mutants
535 that are attenuated during mouse infection using defined pools of Tn mutants and
536 quantification of Tn mutant fitness with deep sequencing. Most genome-wide screens of
537 *M. tuberculosis* Tn mutants in the mouse model used complex Tn mutant pools, which
538 enabled analysis of Tn mutant fitness only in mouse spleens due to a strict colonization
539 bottleneck in the lungs [12-14, 16]. Initial Tn mutant screens conducted with signature-
540 tagged mutagenesis technology used low-complexity Tn mutant pools to identify *M.*
541 *tuberculosis* Tn mutants specifically attenuated in the lungs [17, 73, 74]. A few recent
542 studies have examined fitness of deletion mutants with sequence barcodes and
543 quantification of mutant fitness in the lungs by sequencing [75, 76]. However, to our
544 knowledge this is the first study to use low-complexity Tn mutant pools and Tn-seq to
545 identify *M. tuberculosis* mutants attenuated in mouse lungs. A similar strategy combined
546 with high-dose aerosol infection could be used to identify *M. tuberculosis* genes that are
547 required for aerosol transmission and for fitness within lung tissues.

548 Our work is also the first to determine role of multiple essential central metabolic
549 pathways in *M. tuberculosis* pathogenesis. Our results directly demonstrate that *M.*
550 *tuberculosis* requires both *de novo* Phe synthesis and *de novo* purine/thiamine
551 synthesis for replication and survival in infected mice, implicating these pathways as

552 prime targets for development of new TB drugs. Our Tn-seq screen identified IlvA as a
553 conditionally essential gene that is not required for *M. tuberculosis* survival in the host,
554 suggesting that BCAA biosynthesis pathways should be de-prioritized for drug
555 development. Our screen also revealed several other metabolic pathways, including
556 synthesis of other amino acids (Glu, Pro), PABA and riboflavin that *M. tuberculosis*
557 requires for growth in host tissues. Overall, our results widen the scope of potential
558 targets for TB drug development.
559
560 **MATERIALS AND METHODS**
561 **Bacterial strains and growth conditions.** *M. tuberculosis* Erdman wild-type and
562 derivative strains were grown aerobically at 37°C in Middlebrook 7H9 (Difco) liquid
563 medium supplemented with 10% albumin-dextrose-saline (ADS), 0.5% glycerol, and
564 0.1% Tween-80 or on Middlebrook 7H10 (Difco) agar supplemented with 10% oleic
565 acid-albumin-dextrose-catalase (OADC; BD Biosciences) and 0.5% glycerol unless
566 otherwise noted. Frozen stocks of *M. tuberculosis* strains were made by growing
567 cultures to late-exponential phase, adding glycerol to 15% final concentration, and
568 storing at -80°C. Liquid cultures of M-ES Tn mutants or the M-ES Tn library were grown
569 in MtbYM rich medium (MtbYM) pH 6.6 [27] supplemented with 10% OADC and 0.05%
570 tyloxapol or on MtbYM agar plates [27], unless otherwise noted. Antimicrobials were
571 used at the following concentrations: kanamycin (Kan) 25 µg/ml for agar or 15 µg/ml for
572 liquid, hygromycin (Hyg) 50 µg/ml, cycloheximide 100 µg/ml.
573 **Recovery of Tn mutants from the arrayed Tn mutant library.** Tn mutants were
574 recovered from the mapped location in our arrayed Tn mutant library [28] by streaking
575 on MtbYM agar containing Kan and incubating at 37˚C for at least three weeks. Up to
576 four individual colonies were picked and grown in 10 ml of MtbYM broth containing Kan
577 at 37˚C with aeration. The Tn insertion site was confirmed by PCR using a gene-specific
578 primer 5' or 3' of the TA site and a primer specific to the Tn (**Table S4**) followed by
579 Sanger sequencing of the PCR product. M-ES Tn mutants were screened for secondary
580 point mutations that disrupt PDIM production known to be present in our Tn library by
581 PCR and Sanger sequencing. We screened for mutations in *ppsD* and *ppsE* previously

582 identified in other Tn mutants [28] and for additional common mutations in *ppsB*, *ppsC*
583 and *ppsE* identified by whole-genome sequencing of M-ES Tn mutants (**Table S4**).
584 **Whole genome sequencing.** The whole genome of each M-ES Tn mutant included in
585 the M-ES library was sequenced by short-read Illumina sequencing to identify mutations
586 in the phthiocerol dimycocerosate (PDIM) locus that could result in PDIM deficiency. Tn
587 mutants were grown to an OD_{600} of 1.0 in MtbYM broth; genomic DNA (gDNA) was
588 extracted by the CTAB-lysozyme method [77] and cleaned with the Genomic DNA
589 concentrator and cleanup kit 25 (Zymo). gDNA was submitted to SeqCenter (formerly
590 Microbial Genome Sequencing Center, MiGS) (Pittsburgh, PA) for library preparation
591 and Illumina sequencing (151 bp paired-end output, 400 Mbp, 2.67 M reads per
592 sample). To generate a consensus sequence for each strain, paired reads were mapped
593 to the *M. tuberculosis* Erdman reference genome (NC_020559.1) using the "map to
594 reference" function in Geneious 2021 software (Biomatters, Ltd.) as previously
595 described [28]. To identify single nucleotide polymorphisms (SNPs) in Tn mutant
596 genomes, the WT Erdman and Tn mutant consensus sequences were aligned in
597 Geneious using the "Align Whole Genomes" function with the default Mauve Genome
598 parameters, as described [28]. Tn mutant genomes were only examined for SNPs in the
599 PDIM locus (*tesA* – *lppX*). SNPs identified in genes required for PDIM synthesis were
600 confirmed by PCR amplification and Sanger sequencing (**Table S4**). Tn mutants with
601 confirmed SNPs in the PDIM locus were excluded from the study. To confirm Tn
602 insertion sites in the Tn mutants, reads were mapped to the *Himar1* Tn sequence in
603 Geneious as described above and sequences adjacent to the Tn were compared to the
604 *M. tuberculosis* Erdman reference genome. Mutants with more than one Tn insertion
605 were excluded from the study.
606 **Creation and screening of the M-ES Tn library by Tn-seq.** We created our M-ES Tn
607 mutant library using Tn mutants in genes predicted to be conditionally essential in
608 Middlebrook 7H9 medium but not MtbYM rich medium (M-ES genes) [11, 27], with a
609 single Tn insertion and no mutations in the PDIM locus based on whole-genome
610 sequencing (**Table S1**). For positive controls, we isolated Tn mutants in genes known to
611 be required for *M. tuberculosis* virulence (*panC*::Tn and *phoP*::Tn) [29, 36, 37]. For
612 negative controls, we isolated Tn mutants in genes known to be dispensable during

613 mouse infection (*rpfA*::Tn, *rpfE*::Tn, *tadA*::Tn, *pstB*::Tn, *pstC1*::Tn) [38-40]. Each Tn
614 mutant was grown individually in MtbYM broth until late-logarithmic phase (OD_{600} ~1.0)
615 and mixed in equal abundance to make the M-ES Tn library. Frozen stocks of the M-ES
616 Tn library were made by adding glycerol to 15% final concentration and freezing 1 ml
617 aliquots. The remaining Tn library culture was aliquoted into three 10 ml cultures and
618 pelleted by centrifugation (4100 x*g*, 10 min) for gDNA extraction as a total library
619 (Library) control. For the Tn-seq screen, the Tn library was grown from a frozen stock to
620 mid-exponential phase (OD_{600} = 0.5) in MtbYM broth, washed once with PBS containing
621 0.05% Tween-80 (PBS-T), and resuspended at OD_{600} = 0.05 in PBS-T. Three 9 ml
622 samples of the diluted M-ES Tn library (~10^7 CFU) were pelleted by centrifugation (4100
623 x*g*, 10 min) for gDNA extraction as an input (Liquid) control. The diluted M-ES Tn library
624 was serially diluted and plated on MtbYM agar to enumerate total bacterial CFU and to
625 isolate a plated input (Plate) control.
626 C57BL/6J mice 7 weeks of age were purchased from Jackson Laboratory, USA.
627 Mice were injected with 200 μl of the diluted M-ES Tn library (~2 x10^5 CFU) via the
628 lateral tail vein to deliver ~10,000 CFU to the mouse lungs. Groups of mice (*n*=3) were
629 euthanized by CO_2 overdose at days 1, 7, 21, and 42 post-infection. Lungs and spleens
630 were collected, homogenized in PBS-T, serially diluted, and plated on MtbYM agar
631 containing Kan and cycloheximide to enumerate total bacterial CFU in the sample and
632 to recover at least 10^4 CFU per plate for Tn-seq analysis. Plates were incubated at 37˚C
633 with 5% CO_2 until the biomass on the agar was confluent, up to four weeks. Plates with
634 at least 10^4 CFU for the Plate controls and mouse tissue homogenates were flooded
635 with 2 ml of GTE buffer [77], and gently scraped with a plastic 10 μl loop to loosen the
636 biomass. Bacteria were collected by centrifugation (4100 x*g*, 10 min). Genomic DNA
637 was extracted from all input controls (Library, Liquid, Plate) and from plated mouse lung
638 and spleen homogenate samples by the CTAB-lysozyme method [77], cleaned with the
639 Genomic DNA clean and concentrator kit (Zymo), and submitted to the University of
640 Minnesota Genomics Center (UMGC) for Tn-seq library preparation and Illumina
641 sequencing.
642 **Transposon sequencing (Tn-seq) and data analysis.** Tn-seq was performed as
643 previously described [27]. *M. tuberculosis* gDNA was fragmented with a Covaris S220

644 ultrasonicator and a whole genome library was prepared using the TruSeq Nano library
645 preparation kit (Illumina). Library fragments containing Tn junctions were PCR-amplified
646 from the whole genome library using the Tn-specific primer Mariner_1R_TnSeq_noMm
647 and Illumina p7 primer (**Table S4**). The amplified products were uniquely indexed to
648 allow sample pooling and multiplexed sequencing. A total of 27 Mariner-enriched Tn-seq
649 libraries were created. All libraries were pooled and sequenced on a NextSeq 2K P1
650 2x150-bp run (Illumina) with 20% PhiX target spiked in to account for the low diversity of
651 Tn-seq libraries. Approximately 117 M pass filter reads were generated for the lane. All
652 expected barcodes were detected and reads were balanced (Mean reads ≈ 2.5 M) with
653 mean quality scores for all libraries ≥Q30.
654 Tn-seq analysis was done as previously described [28]. Sequencing reads were
655 filtered to remove reads without the Tn sequence "GGACTTATCAGCCAACCTGT". The
656 5' Illumina adaptor sequences were trimmed using BBDuk
657 (https://sourceforge.net/projects/bbmap/). Each trimmed read was cut to 30 bases and
658 sequences not starting with TA were removed. Remaining reads were mapped to the *M.*
659 *tuberculosis* Erdman genome (NC_020559.1) using HISAT2. Mapped reads were
660 counted at each TA insertion site to generate read count tables for TnseqDiff analysis.
661 TnseqDiff normalized the read counts using the default trimmed mean of M values
662 (TMM) normalization method [78, 79], and then determined conditional essentiality for
663 each TA insertion site between experimental conditions. TnseqDiff calculated the fold
664 change and corresponding two-sided *P*-value for each TA insertion site [41]. All *P*-values
665 were adjusted for multiple testing using the Benjamini-Hochberg procedure in TnseqDiff.
666 The cut-off values for statistical significance were set at a fold-change of > $\log_2$ ±2 and
667 an adjusted *P*-value < 0.025.
668 **Tn mutant complementation.** Complementation vectors pMV-*purF* and pMV-*pheA*
669 were in made in the integrating plasmid pMV306hyg [28] by Gibson assembly. Each
670 gene was PCR-amplified (Phusion; New England Biolabs) along with ~300 bases 5' of
671 the translation start site to include the native promoter using primers designed with 16-
672 20 bases complementary to the gene of interest and 18-22 bases that overlap the NcoI
673 site in pMV306hyg (**Table S4**). PCR products were purified (Qiagen PCR purification kit)
674 and assembled with pMV306hyg that was linearized by digestion with NcoI using HiFi

675 DNA Assembly Master Mix (New England Biolabs) according to the manufacturer's
676 instructions followed by Sanger sequencing of the cloned gene. The *purF*::Tn and
677 *pheA*::Tn mutants were electroporated with the corresponding complementation vector
678 as described [80]. Each Tn mutant was grown in 7H9 with the appropriate supplements
679 added (60 μM thiamine and 150 μM hypoxanthine for *purF*::Tn or 0.5% casamino acids
680 for *pheA*::Tn). Transformants were selected on Middlebrook 7H10 agar containing Kan
681 and Hyg without supplements. The complementing plasmid was confirmed by PCR
682 (**Table S4**).
683 **Growth curves.** Each M-ES Tn mutant in the M-ES Tn library and WT Erdman were
684 grown individually in MtbYM broth to mid-exponential phase (OD_{600} = 0.4-0.6), pelleted
685 by centrifugation (2850 x*g*, 10 min) and washed three times with PBS-T before diluting
686 to OD_{600} = 0.01 in 7H9. Optical density (OD_{600}) was measured every 2-3 days.
687 To confirm conditional essentiality of *purF*::Tn in 7H9, WT, *purF*::Tn and *purF*::Tn
688 pMV-*purF* were grown to mid-exponential phase (OD_{600} = 0.4-0.6) in 7H9 supplemented
689 with 60 μM thiamine and 150 μM hypoxanthine (7H9 +thiam +hypo), pelleted by
690 centrifugation (2850 x*g*, 10 min) and washed three times with PBS-T before diluting to
691 OD_{600} = 0.01 in 7H9 or 7H9 +thiam +hypo. The OD_{600} was measured every 2-3 days.
692 Surviving bacteria were enumerated by serially diluting in PBS-T and plating on
693 Middlebrook 7H10 agar with 10% OADC and 0.5% glycerol. 7H10 agar was additionally
694 supplemented with 60 μM thiamine and 150 μM hypoxanthine for recovery of the
695 *purF*::Tn mutant. At later time points, bacteria in 1 ml of the *purF*::Tn 7H9 culture were
696 collected by centrifugation (3000 x*g*, 10 min), resuspended in 100 μl of PBS-T and
697 plated. Plates were incubated for at least 4 weeks at 37˚C before enumerating CFU.
698 To confirm conditional essentiality of *pheA*::Tn in 7H9, WT, *pheA*::Tn and
699 *pheA*::Tn pMV-*pheA* were grown to mid-exponential phase (OD_{600} = 0.4-0.6) in 7H9
700 supplemented with 0.5% casamino acids (7H9 +cas), pelleted by centrifugation (2850
701 x*g*, 10 min) and washed three times with PBS-T before diluting to OD_{600} = 0.01 in 7H9 or
702 7H9 +cas. The OD_{600} was measured every 2-3 days. Surviving bacteria were
703 enumerated by serially diluting in PBS-T and plating on Middlebrook 7H10 agar with
704 10% OADC and 0.5% glycerol. 7H10 agar was additionally supplemented with 0.5%

705 casamino acids for recovery of the *pheA*::Tn mutant. Plates were incubated for at least
706 4 weeks at 37˚C before enumerating CFU.
707 **Phthiocerol dimycocerosate (PDIM) labeling and detection.** PDIM production was
708 measured by a radiolabeling and thin layer chromatography (TLC) method [81].
709 Cultures grown to mid-logarithmic phase in 10 ml of 7H9 broth with appropriate
710 supplements (7H9 +thiam +hypo for *purF*::Tn, 7H9 +cas for *pheA*::Tn) were labeled for
711 48 hr with 10 µCi of [1-^{14}C] propionic acid, sodium salt (American Radiolabeled
712 Chemicals, Inc; specific activity 50-60 mCi/mmol) prior to apolar lipid extraction and
713 detection of the PDIM lipid by TLC as described [28].
714 **Mouse aerosol infection.** For retesting individual Tn mutant and complemented
715 strains, male and female C57BL/6J mice 6-8 weeks of age were purchased from
716 Jackson Laboratory, USA, and infected via the aerosol route using an Inhalation
717 Exposure System (GlasCol) as described [82]. The nebulizer was loaded with a
718 bacterial suspension in PBS-T at OD_{600} = 0.007 for WT and complemented strains or
719 OD_{600} = 0.01 for the *purF*::Tn or *pheA*::Tn mutant strains to deliver ~100 CFU to the
720 lungs. Groups of mice (*n* = 6, 3 female and 3 male) were euthanized by CO_2 overdose
721 at 1, 7, 21, and 42 days post-infection. Bacterial CFU were enumerated by plating
722 serially diluted lung and spleen homogenates on 7H10 agar with cycloheximide. The
723 7H10 agar was supplemented with 60 µM thiamine and 150 µM hypoxanthine for
724 recovery of the *purF*::Tn mutant or with 0.5% casamino acids for recovery of the
725 *pheA*::Tn mutant. Colonies were counted after at least 4 weeks of incubation at 37˚C.
726 **Animal ethics statement.** All animal protocols used in this study were reviewed and
727 approved by the University of Minnesota Institutional Animal Care and Use Committee
728 (IACUC) under protocol numbers 1912-37660A and 2210-40465A. The University of
729 Minnesota's NIH Animal Welfare Assurance Number is D16-00288 (A3456-01),
730 expiration date 04/30/2024. All animal experiments were done in strict accordance with
731 the recommendations in the Guide for the Care and Use of Laboratory Animals of the
732 National Institutes of Health [83].
733 **Statistical analysis.** A student's unpaired t-test (two-tailed) was used for pairwise
734 comparisons between WT, mutant and complemented strains. *P* values were calculated

using GraphPad Prism 8.0 (GraphPad Software, Inc). P values < 0.05 were considered statistically significant.

Custom scripts and code. All custom scripts and R code used for Illumina sequence read processing are available at https://github.com/bloc0078/umn-tischler-tnseq. Custom R code used for TnseqDiff analysis is provided in the supplementary material **S1 Files**.

Data availability. All raw sequencing data from whole genome sequencing and Tn-seq experiments underlying the results reported are publicly available in FASTA format at the NCBI Sequence Read Archive (BioProject PRJNA1006392). All raw numerical and image data underlying the figures are provided in the supplementary materials.

ACKNOWLEDGEMENTS

This work was completed in part with resources, including instrumentation and staff, at the University of Minnesota Genomics Center (UMGC; RRIC SCR_012413) and the University of Minnesota Imaging Centers (UIC: RRID SCR_020997). We thank Drs. Yusuke Minato and Anthony Baughn for developing the custom MtbYM rich media and for helpful discussions. We thank Dr. Lili Zhao for providing the updated R code for TnseqDiff analysis.

REFERENCES

1. WHO. Global tuberculosis report 2022. Geneva: World Health Organization; 2022.
2. WHO. WHO consolidated guidlines on tuberculosis. Module 4: treatment - drug-susceptible tuberculosis treatment. Geneva: World Health Organization; 2022.
3. WHO. WHO consolidated guidelines on tuberculosis. Module 4: treatment - drug-resistant tuberculosis treatment, 2022 update. Geneva: World Health Organization; 2022.
4. Dorman SE, Nahid P, Kurbatova EV, Phillips PPJ, Bryant K, Dooley KE, et al. Four-month rifapentine regimens with or without moxifloxacin for tuberculosis. N Engl J Med. 2021;384:1705-18.
5. Conradie F, Diacon AH, Ngubane N, Howell P, Everitt D, Crook AM, et al. Treatment of highly drug-resistant pulmonary tuberculosis. N Engl J Med. 2020;382:893-902.
6. Conradie F, Bagdasaryan TR, Borisov S, Howell P, Mikiashvili L, Ngubane N, et al. Bedaquiline-Pretomanid-Linezolid regimens for drug-resistant tuberculosis. N Engl J Med. 2022;387:810-23.

7. Kadura S, King N, Nakhoul M, Zhu H, Theron G, Köser CU, et al. Systematic review of mutations associated with resistance to the new and repurposed *Mycobacterium tuberculosis* drugs bedaquiline, clofazimine, linezolid, delamanid and pretomanid. J Antimicrob Chemother. 2020;75:2031-43.
8. Johnson EO, LaVerriere E, Office E, Stanley M, Meyer E, Kawate T, et al. Large-scale chemical-genetics yields new *M. tuberculosis* inhibitor classes. Nature. 2019;571:72-8.
9. Bosch B, DeJesus MA, Poulton NC, Zhang W, Engelhart CA, Zaveri A, et al. Genome-wide gene expression tuning reveals diverse vulnerabilities of *M. tuberculosis*. Cell. 2021;184:4579-92.
10. Tomasi FG, Rubin EJ. Failing upwards: Genetics-based strategies to improve antibiotic discovery and efficacy in *Mycobacterium tuberculosis*. Front Cell Infect Microbiol. 2022;12:932556.
11. DeJesus MA, Gerrick ER, Xu W, Park SW, Long JE, Boutte CC, et al. Comprehensive essentiality analysis of the *Mycobacterium tuberculosis* genome via saturating transposon mutagenesis. mBio. 2017;8:e02133-16.
12. Sassetti CM, Rubin EJ. Genetic requirements for mycobacterial survival during infection. Proc Natl Acad Sci USA. 2003;100:12989-94.
13. Zhang YJ, Reddy MC, Ioerger TR, Rothchild AC, Dartois V, Schuster BM, et al. Tryptophan biosynthesis protects mycobacteria from CD4 T-cell-mediated killing. Cell. 2013;155:1296-308.
14. Nambi S, Long JE, Mishra BB, Baker R, Murphy KC, Olive AJ, et al. The oxidative stress network of *Mycobacterium tuberculosis* reveals coordination between radical detoxification systems. Cell Host Microbe. 2015;17:829-37.
15. Payros D, Alonso H, Malaga W, Volle A, Mazeres S, Dejean S, et al. Rv0180c contributes to *Mycobacterium tuberculosis* cell shape and to infectivity in mice and macrophages. PLoS Pathog. 2021;17:e1010020.
16. Smith CM, Baker RE, Proulx MK, Mishra BB, Long JE, Park SW, et al. Host-pathogen genetic interactions underlie tuberculosis susceptiblity in genetically diverse mice. eLife. 2022;11:e74419.
17. Cox JS, Chen B, McNeil M, Jacobs WRJ. Complex lipid determines tissue-specific replication of *Mycobacterium tuberculosis* in mice. Nature. 1999;402:79-83.
18. Berney M, Berney-Meyer L, Wong KW, Chen B, Chen M, Kim J, et al. Essential roles of methionine and S-adenosylmethionine in the autarkic lifestyle of *Mycobacterium tuberculosis*. Proc Natl Acad Sci USA. 2015;112:10008-13.
19. Tiwari S, van Tonder AJ, Vilcheze C, Mendes V, Thomas SE, Malek A, et al. Arginine-deprivation-induced oxidative damage sterlizes *Mycobacterium tuberculosis*. Proc Natl Acad Sci USA. 2018;115:9779-84. doi: doi: 10.1073/pnas.1808874115.
20. Smith DA, Parish T, Stoker NG, Bancroft GJ. Characterization of auxotrophic mutants of *Mycobacterium tuberculosis* and their potential as vaccine candidates. Infect Immun. 2001;69:1142-50.
21. Wellington S, Nag PP, Michalska K, Johnston SE, Jedrzejczak RP, Kaushik VK, et al. A small-molecule allosteric inhibitor of *Mycobacterium tuberculosis* tryptophan synthase. Nat Chem Biol. 2017;13:943-50.

815 22. Evans JC, Trujillo C, Wang Z, Eoh H, Ehrt S, Schnappinger D, et al. Validation of
816 CoaBC as a bactericidal target in the coenzyme A pathway of *Mycobacterium*
817 *tuberculosis*. ACS Infect Dis. 2016;2:958-68.
818 23. Park SW, Klotzsche M, Wilson DJ, Boshoff HI, Eoh H, Manjunatha U, et al.
819 Evaluating the sensitivity of *Mycobacterium tuberculosis* to biotin deprivation using
820 regulated gene expression. PLoS Pathog. 2011;7:e1002264.
821 24. Korte J, Alber M, Trujillo CM, Syson K, Kollwer-Brandl H, Deenen R, et al.
822 Trehalose-6-phosphate-mediated toxicity determines essentiality of OtsB2 in
823 *Mycobacterium tuberculosis in vitro* and in mice. PLoS Pathog. 2016;12:e1006043.
824 25. Boshoff HIM, Xu X, Tahlan K, Dowd CS, Pethe K, Camacho LR, et al.
825 Biosynthesis and recycling of nicotinamide cofactors in *Mycobacterium tuberculosis*: an
826 essential role for NAD in nonreplicating bacilli. J Biol Chem. 2008;283:19329-41.
827 26. Vilcheze C, Weinrick B, Wong KW, Chen B, Jacobs WR, Jr. NAD+ auxotrophy is
828 bacteriocidal for the tubercle bacilli. Mol Microbiol. 2010;76:365-77.
829 27. Minato Y, Gohl DM, Thiede JM, Chacón JM, Harcombe WR, Maruyama F, et al.
830 Genomewide assessment of *Mycobacterium tuberculosis* conditionally essential
831 metabolic pathways. mSystems. 2019;4:e00070-19.
832 28. Block AM, Namugenyi SB, Palani NP, Brokaw AM, Zhang L, Beckman KB, et al.
833 *Mycobacterium tuberculosis* requires the outer membrane lipid phthiocerol
834 dimycocerosate for starvation-induced antibiotic tolerance. mSystems. 2023;8:e00699-
835 22.
836 29. Sambandamurthy VK, Wang X, Chen B, Russell RG, Derrick S, Collins FM, et al.
837 A pantothenate auxotroph of *Mycobacterium tuberculosis* is highly attenuated and
838 protects mice against tuberculosis. Nat Med. 2002;8:1171-4.
839 30. Gee CL, Papavinasasundaram KG, Blair SR, Baer CE, Falick AM, King DS, et al.
840 A phosphorylated pseudokinase complex controls cell wall synthesis in mycobacteria.
841 Sci Signal. 2012;5:ra7.
842 31. Shamma F, Rego EH, Boutte CC. Mycobacterial serine/threonine phosphatase
843 PstP is phosphoregulated and localized to mediate control of cell wall metabolism. Mol
844 Microbiol. 2022;118:47-60.
845 32. Jain P, Malakar B, Khan MZ, Lochab S, Singh A, Nandicoori VK. Delineating
846 FtsQ-mediated regulation of cell division in *Mycobacterium tuberculosis*. J Biol Chem.
847 2018;293:12331-49.
848 33. Miyoshi-Akiyama T, Matsumura T, Iwai H, Funatogawa K, Kirikae T. Complete
849 annotated genome sequence of *Mycobacterium tuberculosis* Erdman. J Bacteriol.
850 2012;194:2770.
851 34. Sasindran SJ, Saikolappan S, Scofield VL, Dhandayuthapani S. Biochemical and
852 physiological characterization of the GTP-binding protein Obg of *Mycobacterium*
853 *tuberculosis*. BMC Microbiol. 2011;11:43.
854 35. Kint C, Verstraeten N, Hofkens J, Fauvert M, Michiels J. Bacterial Obg proteins:
855 GTPases at the nexus of protein and DNA synthesis. Crit Rev Microbiol. 2014;40:207-
856 24.
857 36. Pérez E, Samper S, Bordas Y, Guilhot C, Gicquel B, Martín C. An essential role
858 for *phoP* in *Mycobacterium tuberculosis* virulence. Mol Microbiol. 2001;41:179-87.

859 37. Walters SB, Dubnau E, Kolesnikova I, Laval F, Daffé M, Smith I. The
860 *Mycobacterium tuberculosis* PhoPR two-component system regulates genes essential
861 for virulence and complex lipid biosynthesis. Mol Microbiol. 2006;60:312-30.
862 38. Tufariello JM, Jacobs WR, Jr., Chan J. Individual *Mycobacterium tuberculosis*
863 resuscitation-promoting factor homologues are dispensable for growth in vitro and in
864 vivo. Infect Immun. 2004;72:515-26.
865 39. Tischler AD, Leistikow RL, Ramakrishnan P, Voskuil MI, McKinney JD.
866 *Mycobacterium tuberculosis* phosphate uptake system component PstA2 is not required
867 for gene regulation or virulence. PLoS One. 2016;11:e0161467.
868 40. Mann KM, Pride AC, Flentie K, Kimmey JM, Weiss LA, Stallings CL. Analysis of
869 the contribution of MTP and the predicted Flp pilus genes to *Mycobacterium*
870 *tuberculosis* pathogenesis. Microbiol. 2016;162:1784-96.
871 41. Zhao L, Anderson MT, Wu W, Mobley HL, Bachman MA. TnseqDiff: Identification
872 of conditionally essential genes in transposon sequencing studies. BMC Bioinformatics.
873 2017;18:326.
874 42. Zhang Y, Morar M, Ealick SE. Structural biology of the purine biosynthetic
875 pathway. Cell Mol Life Sci. 2008;65:3699-724.
876 43. Warner DF, Evans JC, Mizrahi V. Nucleotide metabolism and DNA replication.
877 Microbiol Spectr. 2014;2:MGM2-0001-2013.
878 44. Parthsarathy A, Cross PJ, Dobson RCJ, Adams LE, Savka MA, Hudson AO. A
879 three-ring circus: metabolism of the three proteogenic aromatic amino acids and their
880 role in the health of plants and animals. Front Mol Biosci. 2018;5:29.
881 45. Prakash P, Pathak N, Hasnain SE. *pheA* (Rv3838c) of *Mycobacterium*
882 *tuberculosis* encodes an allosterically regulated monofunctional prephanate
883 dehydratase that requires both catalytic and regulatory domains for optimum activity. J
884 Biol Chem. 2005;280:20666-71.
885 46. Prakash P, Aruna B, Sardesai AA, Hasnain SE. Purified recombinant hypothetical
886 protein coded by open reading frame Rv1885c of *Mycobacterium tuberculosis* exhibits a
887 monofunctional AroQ class of periplasmid chorismate mutase activity. J Biol Chem.
888 2005;280:19641-8.
889 47. Sasso S, Ramakrishnan C, Gamper M, Hilvert D, Kast P. Characterization of the
890 secreted chorismate mutase from the pathogen *Mycobacterium tuberculosis*. FEBS J.
891 2005;272:375-89.
892 48. Kim S-K, Reddy SK, Nelson BC, Vasquez GB, Davis AS, Howard AJ, et al.
893 Biochemical and structural characterization of the secreted chorismate mutase
894 (Rv1885c) from *Mycobacterium tuberculosis* H37Rv: an *AroQ enzyme not regulated by
895 the aromatic amino acids. J Bacteriol. 2006;188:8638-48.
896 49. Lim J, Lee JJ, Lee S-K, Kim SH, Eum S-Y, Eoh H. Phosphoenolpyruvate
897 depletion mediates both growth arrest and drug tolerance of *Mycobacterium*
898 *tuberculosis* in hypoxia. Proc Natl Acad Sci USA. 2021;118:e2105800118.
899 50. Graindorge M, Giustini C, Kraut A, Moyet L, Curien G, Matringe M. Three
900 different classes of aminotransferases evolved prephenate aminotransferase
901 functionality in arogenate-competent microorganisms. J Biol Chem. 2014;289:3198-208.
902 51. Shukla S, Rao RN, Bhuktar H, Edwin RE, Jamma T, Medishetti R, et al. Wang
903 resin catalysed sonochemical synthesis of pyrazolo [4,3-*d*] pyrimidinones and 2,3

904 dihydroquinazolin-4(1*H*)-ones: Identification of chorismate mutase inhibitors having
905 effects on *Mycobacterium tuberculosis* cell viability. Bioorgan Chem. 2023;134:106542.
906 52. Alokam R, Jeankumar VU, Sridevi JP, Matikonda SS, Peddi S, Alvala M, et al.
907 Identification and structure-activity relationship study of carvacrol derivatives as
908 *Mycobacterium tuberculosis* chorismate mutase inhibitors. J Enzyme Inhib Med Chem.
909 2014;29:547-54.
910 53. Jeankumar VU, Alokam R, Sridevi JP, Suryadevara P, Matikonda SS, Peddi S, et
911 al. Discovery and structure optimization of a series of isatin derivatives as
912 *Mycobacterium tuberculosis* chorismate mutase inhibitors. Chem Biol Drug Dis.
913 2014;83:498-506.
914 54. Goncheva MI, Chin D, Heinrichs DE. Nucleotide biosynthesis: the base of
915 bacterial pathogenesis. Trends Microbiol. 2022;30:793-804.
916 55. Jackson M, Phalen SW, Lagranderie M, Ensergueix D, Chavarot P, Marchal G, et
917 al. Persistence and protective efficacy of a *Mycobacterium tuberculosis* auxotroph
918 vaccine. Infect Immun. 1999;67:2867-73.
919 56. Singh V, Donini S, Pacitto A, Sala C, Hartkoorn RC, Dhar N, et al. The inosine
920 monophosphate dehydrogenase, GuaB2, is a vulnerable new bactericidal drug target
921 for tuberculosis. ACS Infect Dis. 2017;3:5-17.
922 57. Zhang Z, Caradoc-Davies TT, Dickson JM, Baker EN, Squire CJ. Structures of
923 glycinamide ribonucleotide transformylase (PurN) from *Mycobacterium tuberculosis*
924 reveal a novel dimer with relevance to drug discovery. J Mol Biol. 2009;389:722-33.
925 58. Le Nours J, Bulloch EMM, Zhang Z, Greenwood DR, Middleditch MJ, Dickson
926 JMJ, et al. Structural analyses of a purine biosynthetic enzyme from *Mycobacterium*
927 *tuberculosis* reveal a novel bound nucleotide. J Biol Chem. 2011;286:40706-16.
928 59. Chen C, Liu Z, Liu L, Wang J, Jin Q. Structural characterization of glycinamide-
929 RNase-transformylase T from *Mycobacterium tuberculosis*. Emerg Microbes Infect.
930 2020;9:58-66.
931 60. Charoensutthivarakul S, Thomas SE, Curran A, Brown KP, Belardinelli JM,
932 Whitehouse AJ, et al. Development of inhibitors of SAICAR synthetase (PurC) from
933 *Mycobacterium abscessus* using a fragment-based approach. ACS Infect Dis.
934 2022;8:296-309.
935 61. Park Y, Pacitto A, Bayliss T, Cleghorn LAT, Wang Z, Hartman T, et al. Essential
936 but not vulnerable: indazole sulfonamides targeting inosine monophosphate
937 dehydrogenase as potential leads against *Mycobacterium tuberculosis*. ACS Infect Dis.
938 2017;3:18-33.
939 62. Du Q, Wang H, Xie J. Thiamin (vitamin B1) biosynthesis and regulation: a rich
940 source of anti-microbial drug targets? Int J Biol Sci,. 2011;7:41-52.
941 63. Zilles JL, Croal LR, Downs DM. Action of the thiamine antagonist bacimethrin on
942 thiamine biosynthesis. J Bacteriol. 2000;182:5606-10.
943 64. Kim HJ, Lee H, Lee Y, Choi I, Ko Y, Lee S, et al. The ThiL enzyme is a valid
944 antibacterial target essential for both thiamine biosynthesis and salvage pathways in
945 *Pseudomonas aeruginosa*. J Biol Chem. 2020;295:10081-91.
946 65. Khare G, Kar R, Tyagi AK. Identification of inhibitors against *Mycobacterium*
947 *tuberculosis* thiamin phosphate synthase, an important target for the development of
948 anti-TB drugs. PLoS One. 2011;67:e22441.

949 66. Sasso S, Ökvist M, Roderer K, Gamper M, Codoni G, Krengel U, et al. Structure
950 and function of a complex between chorismate mutase and DAHP synthase: efficiecy
951 boost for the junior partner. EMBO J. 2009;28:2128-42.
952 67. Keer J, Smeulders MJ, Williams HD. A *purF* mutant of *Mycobacterium smegmatis*
953 has impaired survival during oxygen-starved stationary phase. Microbiol. 2001;147:473-
954 81.
955 68. Thiede JM, Kordus SL, Turman BJ, Buonomo JA, Aldrich CC, Minato Y, et al.
956 Targeting intracellular *p*-aminobenzoic acid production potentiates the anti-tubercular
957 action of antifolates. Sci Rep. 2016;6:38083.
958 69. Sharma R, Keshari D, Singh KS, Singh SK. Biochemical and functional
959 characterization of MRA_1571 of *Mycobacterium tuberculosis* H37Ra and effect of its
960 down-regulation on survival in macrophages. Biochem Biophys Res Commun.
961 2017;487:892-7.
962 70. Amorim Franco TM, Blanchard JS. Bacterial branched-chain amino acid
963 biosynthesis: structures, mechanisms, and drugability. Biochemistry. 2017;56:5849-65.
964 71. Awasthy D, Gaonkar S, Shandil RK, Yadav R, Bharath S, Marcel N, et al.
965 Inactivtion of the *ilvB1* gene in *Mycobacterium tuberculosis* leads to branched-chain
966 amino acid auxotrophy and attenuation of virulence in mice. Microbiol. 2009;155:2978-
967 87.
968 72. Borah K, Beyb M, Theorell A, Wu H, Basu P, Mendum TA, et al. Intracellular
969 *Mycobacterium tuberculosis* exploits multiple host nitrogen sources during growth in
970 human macrophages. Cell Rep. 2019;29:3580-91.
971 73. Camacho LR, Ensergueix D, Perez E, Gicquel B, Guilhot C. Identification of a
972 virulence gene cluster of *Mycobacterium tuberculosis* by signature-tagged transposon
973 mutagenesis. Mol Microbiol. 1999;34:257-67.
974 74. Hisert KB, Kirksey MA, Gomez JE, Sousa AO, Cox JS, Jacobs WRJ, et al.
975 Identification of *Mycobacterium tuberculosis* counterimmune (*cim*) mutants in
976 immunodeficient mice by differential screening. Infect Immun. 2004;72:5315-21.
977 75. Bellerose MM, Proulx MK, Smith CM, Baker RE, Ioerger TR, Sassetti CM.
978 Distinct bacterial pathways influence the efficacy of antibiotics against *Mycobacterium*
979 *tuberculosis*. mSystems. 2020;5:e00396-20.
980 76. Koh E-I, Oluoch PO, Ruecker N, Proulx MK, Soni V, Murphy KC, et al. Chemical-
981 genetic interaction mapping links carbon metabolism and cell wall structure to
982 tuberculosis drug efficacy. Proc Natl Acad Sci USA. 2022;119:e2201632119.
983 77. Larsen MH, Biermann K, Tandberg S, Hsu T, Jacobs WR, Jr. Genetic
984 manipulation of *Mycobacterium tuberculosis*. Curr Protocols Microbiol. 2007:10A.2.1-
985 A.2.21.
986 78. Robinson MD, McCarthy DJ, Smyth GK. edgeR: a bioconductor package for
987 differential expression analysis of digital gene expression data. Bioinformatics.
988 2010;26:139-40.
989 79. Robinson MD, Oshlack A. A scaling normalization method for differential
990 expression analysis of RNA-seq data. Genome Biol. 2010;11:R25.
991 80. Tischler AD, Leistikow RL, Kirksey MA, Voskuil MI, McKinney JD. *Mycobacterium*
992 *tuberculosis* requires phosphate-responsive gene regulation to resist host immunity.
993 Infect Immun. 2013;81:317-28.

994 81. Kirksey MA, Tischler AD, Siméone R, Hisert KB, Uplekar S, Guilhot C, et al.
995 Spontaneous phthiocerol dimycocerosate-deficient variants of *Mycobacterium*
996 *tuberculosis* are susceptible to gamma interferon-mediated immunity. Infect Immun.
997 2011;79:2829-38.
998 82. Ramakrishnan P, Aagesen AM, McKinney JD, Tischler AD. *Mycobacterium*
999 *tuberculosis* resists stress by regulating PE19 expression. Infect Immun. 2016;84:735-
1000 46.
1001 83. National Research Council. Guide for the care and use of laboratory animals, 8th
1002 ed. Washington, DC: National Academies Press; 2011.
1003
1004 **FIGURE LEGENDS**

1005 **Fig 1. *M. tuberculosis* Tn mutants in genes encoding central metabolic enzymes**
1006 **exhibit growth defects in Middlebrook 7H9 medium.** Wild-type *M. tuberculosis*
1007 Erdman and M-ES Tn mutant strains were grown in MtbYM rich medium, washed twice
1008 in PBS-T, and diluted to OD_{600} = 0.01 in Middlebrook 7H9 medium. Growth was
1009 monitored by measuring the OD_{600}. Tn mutants are grouped according to predicted
1010 function: **(A)** purine and thiamine metabolism (*purF*, *purM*, *purQ*), **(B-C)** amino acid
1011 biosynthesis (*pheA*, *trpB*, *trpG*, *proC*, *gltB*, *ilvA*), **(D)** pantothenate, riboflavin, and *p*-
1012 amino benzoic acid (PABA) biosynthesis (*panC*, *ribA2*, *ribG*, *pabB)*, **(E-F)** Tn insertions
1013 within non-essential gene regions (*pstP, fhaA, ftsQ, ERDMAN_3321*) or misannotated
1014 genes (*ERDMAN_2739, ERDMAN_4254*). Data represent the mean ± standard error of
1015 three biological replicates.

1016 **Fig 2. Tn-seq screen of the *M. tuberculosis* M-ES Tn library identifies multiple**
1017 **central metabolic pathways required for fitness in mice. (A)** M-ES Tn-seq screen
1018 methods. Individual Tn mutants grown in MtbYM rich medium were mixed in equal
1019 abundance to create the M-ES Tn library. Triplicate M-ES Tn library samples were
1020 collected for Tn-seq (Library control) and the remainder was aliquoted and frozen for
1021 experiments. The M-ES Tn library was grown in MtbYM rich broth, then washed and
1022 diluted in PBS-T to OD_{600} = 0.05. Triplicate samples of the diluted M-ES Tn library were
1023 collected (Liquid control) and the diluted M-ES Tn library was plated on MtbYM rich agar
1024 in triplicate (Plate control) for Tn-seq. Mice were injected via the lateral tail vein with
1025 ~10^5 CFU of the M-ES Tn library to seed at least 10^4 CFU in the lungs and spleen. Mice
1026 (*n*=3) were euthanized at days 1, 7, 21, and 42. Lung and spleen homogenates were
1027 plated on MtbYM rich agar to recover surviving Tn mutants for Tn-seq. **(B)** *M.*

1028 *tuberculosis* CFU recovered from lungs (blue) and spleens (green). **(C)** Heat map of $\log_2$
1029 fold change in Tn mutant abundance between the indicated conditions determined by
1030 TnseqDiff analysis of Tn-seq data. Positive values (red) indicate a relative fitness
1031 advantage; negative values (blue) indicate a relative fitness defect. **(D-F)** Volcano plots
1032 of TnseqDiff analysis of Tn-seq data for the M-ES Tn mutant library for **(D)** lungs at day
1033 1 compared to the Plate control; **(E)** lungs at day 21 compared to lungs at day 1; or **(F)**
1034 spleens at day 21 compared to spleens at day 1. Dashed lines indicate cutoffs for
1035 statistical significance of ± 2 $\log_2$ fold change and adjusted *P* value <0.025. Tn mutants
1036 meeting these significance cutoffs are colored and labeled.
1037 **Fig 3. Loss of *purF* causes death of *M. tuberculosis* in the absence of nutrient**
1038 **supplementation *in vitro* and in mice. (A)** Pathway for *de novo* synthesis of purine
1039 nucleotides and thiamine in *M. tuberculosis*. Solid lines indicate a single step; dashed
1040 lines indicate multiple steps. Proteins that catalyze the first five steps are indicated.
1041 Intermediate abbreviations: PPP, pentose phosphate pathway; PRPP, 5-phosphoribosyl
1042 pyrophosphate; PRA, 5-phospho-D-ribosylamine; GAR, 5'-phosphoribosylglycinamide;
1043 FGAR, 5'-phosphoribosyl-N-formylglycinamide; FGAM, 5'-phosphoribosyl N-
1044 formylglycinamidine; AIR, 5-aminoimidazole ribotide. **(B-C)** Strains grown in 7H9
1045 supplemented with 60 μM thiamine and 150 μM hypoxanthine were washed in PBS-T
1046 and diluted to OD_{600} = 0.01 in 7H9 or 7H9 supplemented with 60 μM thiamine and 150
1047 μM hypoxanthine. Bacterial growth and survival were measured by **(B)** optical density at
1048 600 nm or **(C)** serial dilutions and plating to recover viable CFU. **(D-E)** C57BL/6J mice
1049 were infected by the aerosol with the indicated strains. Mice (*n*=6) were euthanized at
1050 days 1, 7, 21, and 42 post-infection. Lung **(D)** and spleen **(E)** homogenates were serially
1051 diluted and plated to recover viable CFU. In **(C-E)**, WT and *purF*::Tn pMV-*purF* were
1052 plated on 7H10 agar; *purF*::Tn was plated on 7H10 agar supplemented with 60 μM
1053 thiamine and 150 μM hypoxanthine. Data represent the mean ± standard error of three
1054 biological replicates **(B-C)** or six animals **(D-E)**. Asterisks indicate *P*-value < 0.05; n.d.
1055 indicates not detected (detection limit = 1 CFU).
1056 **Fig 4. *M. tuberculosis* requires Phe synthesis for survival *in vitro* in the absence**
1057 **of amino acid supplementation and in mice. (A)** Phenylalanine biosynthesis in *M.*
1058 *tuberculosis*. Single arrows represent one-way reactions. Double arrows represent

1059 reversible reactions. Proteins predicted to catalyze each step are indicated. **(B-C)**
1060 Strains grown in 7H9 supplemented with 0.5% casamino acids were washed in PBS-T
1061 and diluted to OD_{600} = 0.01 in 7H9 or 7H9 supplemented with 0.5% casamino acids.
1062 Bacterial growth and survival were measured by **(B)** optical density at 600 nm and **(C)**
1063 serial dilutions and plating to recover viable CFU. **(D-E)** C57BL/6J mice were infected
1064 by aerosol with the indicated strains. Mice (*n*=6) were euthanized at days 1, 7, 21, and
1065 42 post-infection. Lung **(D)** and spleen **(E)** homogenates were serially diluted and plated
1066 to recover viable CFU. In **(C-E)**, WT and *pheA*::Tn pMV-*pheA* were plated on 7H10
1067 agar; *pheA*::Tn was plated on 7H10 agar with 0.5% casamino acids. Data represent the
1068 mean ± standard error of three biological replicates **(B-C)** or six animals **(D-E)**. Asterisks
1069 indicate *P*-value < 0.05; n.d. indicates not detected (detection limit = 1 CFU).
1070
1071 **SUPPORTING INFORMATION**
1072 **S1 Table. *M. tuberculosis* Tn mutants in M-ES genes recovered from an arrayed**
1073 **Tn mutant library.**
1074 **S2 Table. Tn-seq read counts at each Tn insertion site for all experimental**
1075 **conditions.**
1076 **S3 Table. Complete TnseqDiff analysis to identify Tn mutants with differential**
1077 **fitness across experimental conditions.** Comparisons between conditions are
1078 indicated in each tab. Bolded text indicates Tn mutants that met statistical significance
1079 cutoffs ($\log_2$ fold change > ± 2, adjusted *P* value <0.025.
1080 **S4 Table. Oligonucleotide primers.**
1081 **S1 Fig. TnseqDiff analyses to identify Tn mutants with fitness defects in *in vitro***
1082 **input controls and mouse spleens.** Volcano plots of TnseqDiff statistical analyses of
1083 Tn-seq data to determine relative Tn mutant fitness in (**A)** infection input liquid culture
1084 (Liquid) vs. M-ES Tn library control (Library), **(B)** plate recovery of infection culture
1085 (Plate) vs. M-ES Tn library control (Library), **(C)** spleens at day 1 post-infection (D1
1086 Spleen) vs. plated input control (Plate)**, (D)** spleens at day 7 vs. day 1 post-infection,
1087 and **(E)** spleens at day 42 vs. day 1 post-infection. Dashed lines indicate cutoffs for
1088 statistical significance of ± 2 $\log_2$ fold change and adjusted P value of <0.025. Tn
1089 mutants meeting these significance cutoffs are colored and labeled.

1090 **S2 Fig. The *M. tuberculosis purF*::Tn mutant requires exogenous hypoxanthine**
1091 **and thiamine for *in vitro* growth.** Strains were grown in 7H9 supplemented with 60 μM
1092 thiamine and 150 μM hypoxanthine, washed with PBS-T, and diluted to OD_{600} = 0.05 in
1093 7H9 broth (wild-type and *purF*::Tn), 7H9 with 150 μM hypoxanthine (*purF*::Tn
1094 +hypoxanthine), or 7H9 with 60 μM thiamine and 150 μM hypoxanthine (*purF*::Tn
1095 +hypoxanthine +thiamine). Growth was measured by optical density at 600 nm. Data
1096 represent means ± standard errors of biological triplicate cultures.
1097 **S3 Fig. *M. tuberculosis* strains tested individually in mice are PDIM-proficient.**
1098 Thin-layer chromatographic analysis of apolar lipids extracted from cultures of WT
1099 Erdman (1) *purF*::Tn (2), *pheA*::Tn (3), *purF*::Tn pMV-*purF* (4), and *pheA*::Tn pMV-*pheA*
1100 (5) labelled with [^{14}C]-propionate, which is preferentially incorporated into PDIM.
1101 **S1 Data. Supporting data files for all graphical figures.** This supporting data file
1102 includes the individual numerical values used to generate the graphs in Fig 1, Fig 2B,
1103 Fig 2C, Fig 3, Fig 4, and S2 Fig and the results of statistical analyses on these data.
1104 Data for each figure are provided in separate tabs. Raw data used for generating the
1105 volcano plots in Figs 2D-F and S1 Fig are provided in S3 Table.
1106 **S2 Data. Raw images.** The raw images used to generate S3 Fig are provided.
1107 **S1 Files**. **Updated R code for TnseqDiff.**

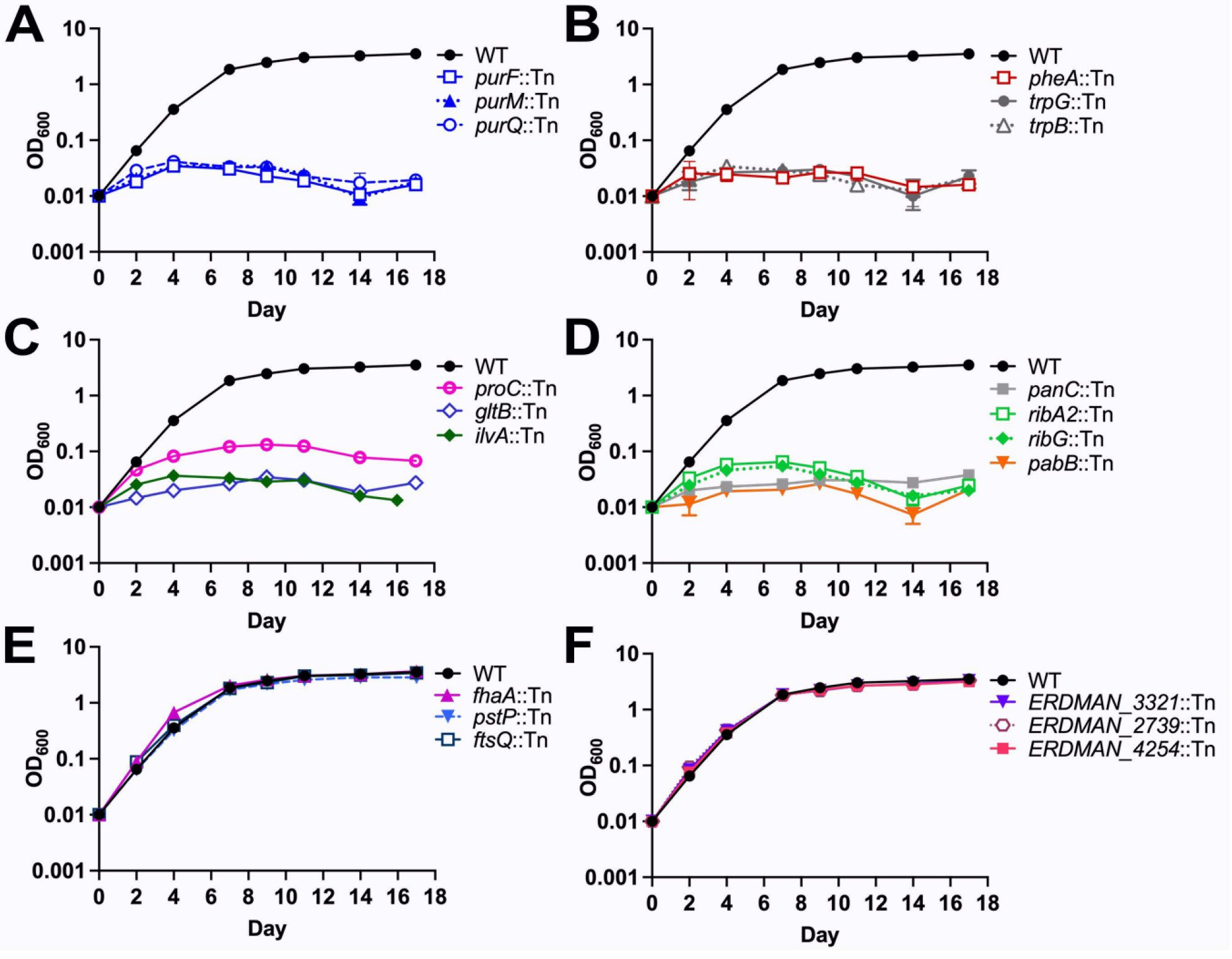
A
B
C
D
E
F
OD600
Day
10
1
0.1
0.01
0.001
0 2 4 6 8 10 12 14 16 18
WT
purF::Tn
purM::Tn
purQ::Tn
pheA::Tn
trpG::Tn
trpB::Tn
proC::Tn
gltB::Tn
ilvA::Tn
panC::Tn
ribA2::Tn
ribG::Tn
pabB::Tn
fhaA::Tn
pstP::Tn
ftsQ::Tn
ERDMAN_3321::Tn
ERDMAN_2739::Tn
ERDMAN_4254::Tn

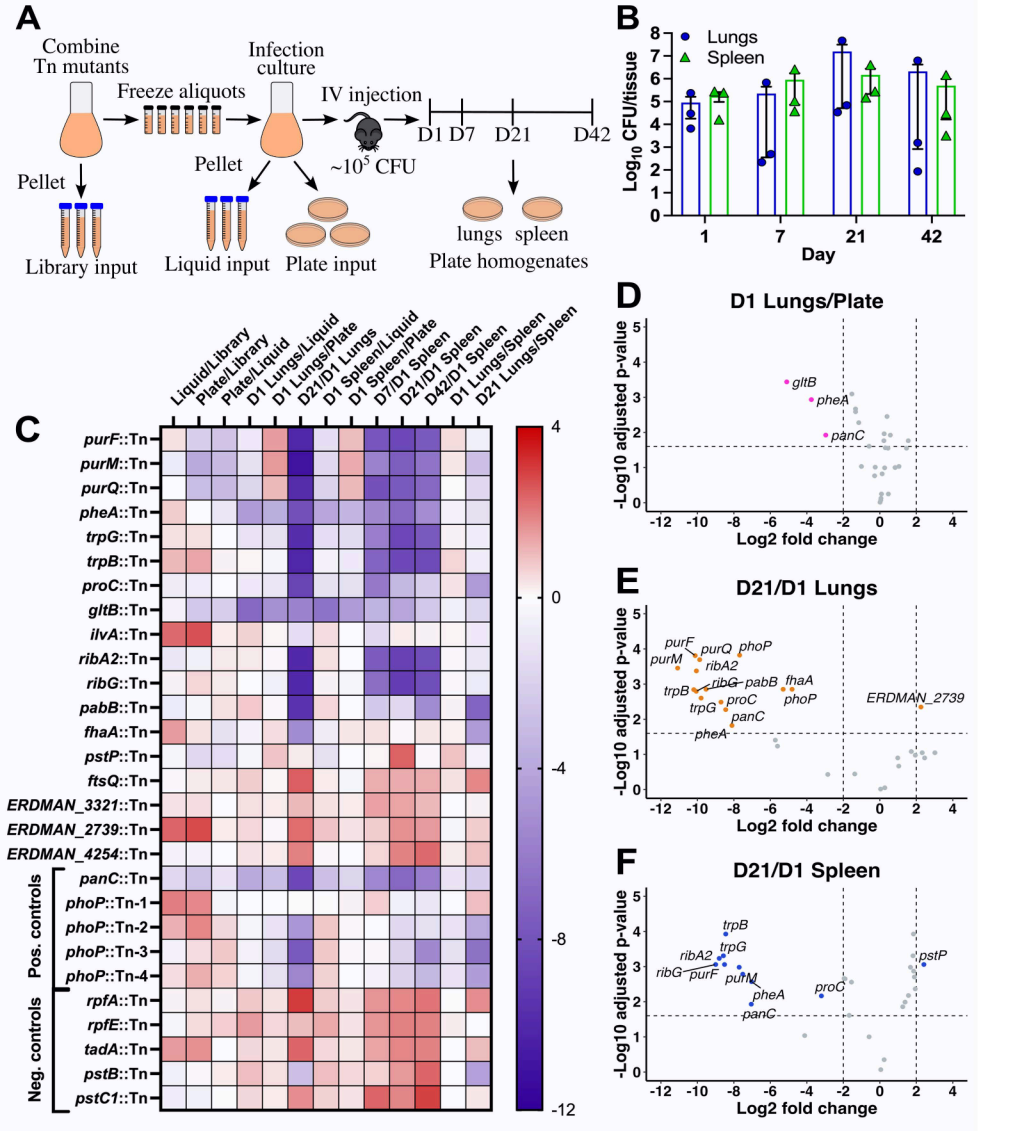
A
Combine Tn mutants
Freeze aliquots
Infection culture
IV injection
~10^5 CFU
D1 D7 D21 D42
Pellet
Pellet
Library input
Liquid input
Plate input
lungs spleen
Plate homogenates
B
Lungs
Spleen
Log10 CFU/tissue
Day
C
Liquid/Library
Plate/Library
Plate/Liquid
D1 Lungs/Liquid
D1 Lungs/Plate
D21/D1 Lungs
D1 Spleen/Liquid
D1 Spleen/Plate
D7/D1 Spleen
D21/D1 Spleen
D42/D1 Spleen
D1 Lungs/Spleen
D21 Lungs/Spleen
purF::Tn
purM::Tn
purQ::Tn
pheA::Tn
trpG::Tn
trpB::Tn
proC::Tn
gltB::Tn
ilvA::Tn
ribA2::Tn
ribG::Tn
pabB::Tn
fhaA::Tn
pstP::Tn
ftsQ::Tn
ERDMAN_3321::Tn
ERDMAN_2739::Tn
ERDMAN_4254::Tn
panC::Tn
phoP::Tn-1
phoP::Tn-2
phoP::Tn-3
phoP::Tn-4
rpfA::Tn
rpfE::Tn
tadA::Tn
pstB::Tn
pstC1::Tn
Pos. controls
Neg. controls
D
D1 Lungs/Plate
-Log10 adjusted p-value
Log2 fold change
gltB
pheA
panC
E
D21/D1 Lungs
purF
purM
purQ
phoP
ribA2
ribG
pabB
fhaA
trpB
trpG
proC
phoP
panC
pheA
ERDMAN_2739
F
D21/D1 Spleen
trpB
trpG
ribA2
ribG
purF
purM
pheA
panC
proC
pstP

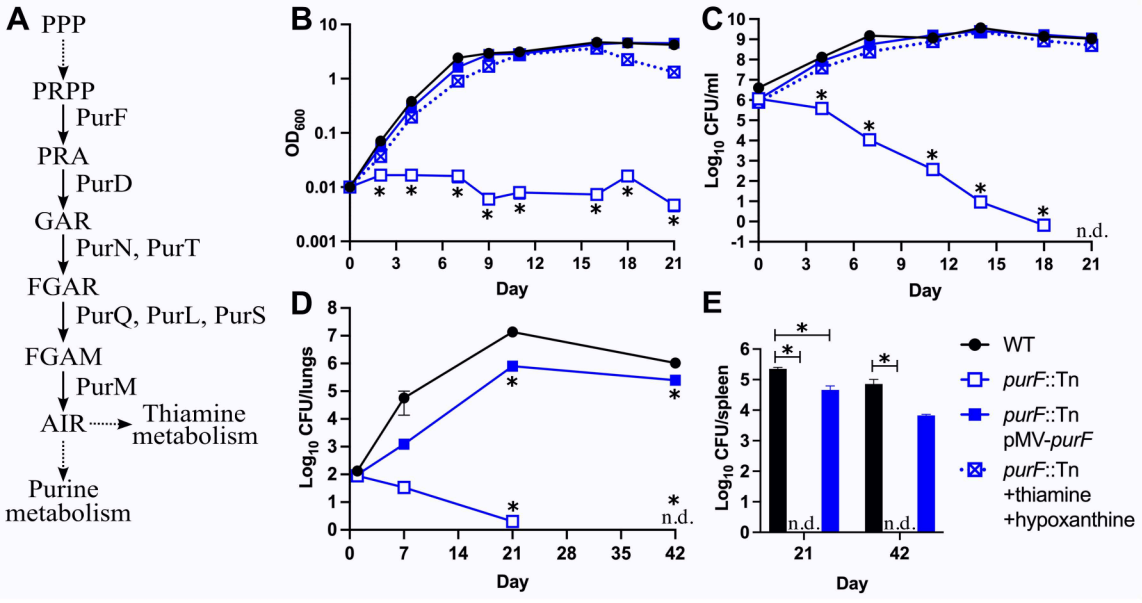
A
PPP
PRPP
PurF
PRA
PurD
GAR
PurN, PurT
FGAR
PurQ, PurL, PurS
FGAM
PurM
AIR
Thiamine metabolism
Purine metabolism
B
OD600
Day
C
Log10 CFU/ml
n.d.
Day
D
Log10 CFU/lungs
n.d.
Day
E
Log10 CFU/spleen
n.d.
n.d.
Day
WT
purF::Tn
purF::Tn pMV-purF
purF::Tn +thiamine +hypoxanthine

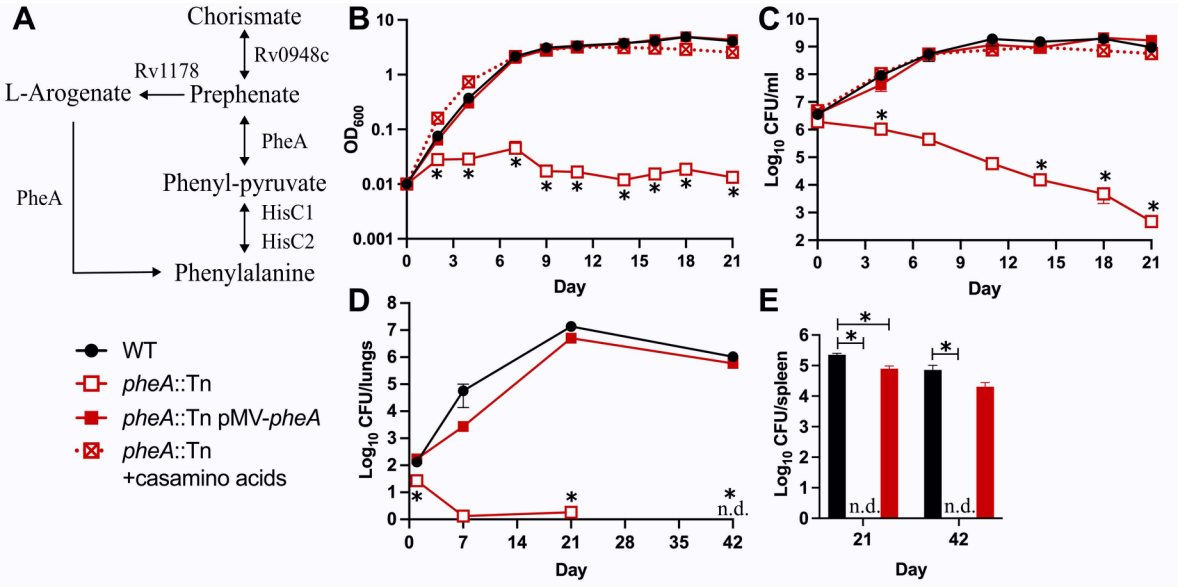
A
Chorismate
Rv0948c
Rv1178
L-Arogenate
Prephenate
PheA
Phenyl-pyruvate
HisC1
HisC2
PheA
Phenylalanine
WT
pheA::Tn
pheA::Tn pMV-pheA
pheA::Tn
+casamino acids
B
OD600
Day
C
Log10 CFU/ml
Day
D
Log10 CFU/lungs
n.d.
Day
E
Log10 CFU/spleen
n.d.
n.d.
Day